JOURNAL OF PETROLOGY

Journal of Petrology, 2015, Vol. 56, No. 10, 2069–2088
doi: 10.1093/petrology/egv066
Original Article

OXFORD

Prograde Metamorphic History of UHP Granulites from the Moldanubian Zone (Bohemian Massif) Revealed by Major Element and Y + REE Zoning in Garnets

R. Jedlicka[1]*, S. W. Faryad[1] and C. Hauzenberger[2]

[1]Institute of Petrology and Structural Geology, Charles University, Prague, 12843, Czech Republic and [2]Institute of Mineralogy and Petrology, Karl-Franzens University, Universitätplatz 2, 8010, Graz, Austria

*Corresponding author. E-mail: radim.jedlicka@natur.cuni.cz

Received December 17, 2014; Accepted October 28, 2015

ABSTRACT

Major and trace element distribution in garnet crystals from felsic granulites of the Kutná Hora Complex provides evidence of two metamorphic events, the first related to continental subduction at ultrahigh-pressure (UHP) conditions and the second to a granulite-facies overprint that occurred at mid- to lower crustal levels. To reconstruct *P–T* paths of both metamorphic events, pseudosection modeling was combined with major and trace element zoning in garnet. The granulites contain lenses and boudins of mantle-derived garnet peridotite and eclogite. UHP conditions are confirmed by the presence of inclusions of micro-diamond and coesite in garnet and zircon in the granulites. Compositional zoning in garnet provides evidence for a pre-granulite-facies high-pressure (HP)–UHP metamorphic history of the rocks. The two distinct metamorphic events are documented by high Y + HREE concentrations in the garnet cores and annuli in the mantle part of the garnet grains. The cores of large garnets with relatively high Ca contents and bell-shaped Mn profiles suggest formation during a prograde low- to medium-temperature metamorphic event that was coeval with HP–UHP metamorphism. Decompression and cooling during exhumation of the rocks led to partial resorption of garnet and release of trace elements into the matrix. The new garnet with high Y + HREE in the annuli was formed during the granulite-facies event at crustal levels.

Key words: granulites; prograde zoning; trace element distribution; UHP; Y + REE

INTRODUCTION

Metamorphism under amphibolite- to granulite-facies conditions in polymetamorphic terranes usually results in the total re-equilibration of minerals and their textures formed during the preceding metamorphic history of the rock. However, garnet, as one of the most refractory phases, may preserve growth or multiple zoning that documents previous metamorphic events (Blackburn & Navarro, 1977; Spear, 1988; Faryad & Chakraborty, 2005; Faryad, 2012). This is due to sluggish intracrystalline diffusional equilibration, where the core of garnet porphyroblasts becomes isolated from the reacting volume of rock during garnet growth. Thus it preserves important information about previous metamorphic evolution (e.g. Carlson, 1989; Chakraborty & Ganguly, 1992; Konrad-Schmolke *et al.*, 2008*a*). Further constraints for multistage or polymetamorphic evolution of basement rocks can be achieved with the use of trace elements, mainly Y + rare earth elements (REE), that are highly compatible within garnet. Their compositional profiles may resist equilibration under granulite-facies conditions owing to slow diffusion rates (Otamendi *et al.*, 2002). Good subjects for testing possible preservation of original major and trace element zoning are felsic granulites in the Bohemian Massif. These granulites contain bodies of high-pressure to

ultrahigh-pressure (HP–UHP) metamorphic rocks, the origin and emplacement of which within the granulite-facies rocks remains uncertain (Faryad, 2011).

The felsic granulites in the Moldanubian Zone are considered as middle or lower crustal rocks that experienced decompression and cooling from maximum pressures of 1·1–1·6 GPa at 800–1000°C (Kotková, 2007, and references therein). Some researchers (e.g. Jakeš, 1997; Kotková & Harley, 1999) postulated their formation by crystallization from a melt at high-pressure conditions. Based on mineral inclusions, compositional zoning of garnet and *P–T* calculations, Faryad *et al.* (2010*b*) suggested that prograde eclogite-facies metamorphism affected these rocks prior to a granulite-facies overprint. This hypothesis was supported by the presence of HP–UHP mafic and ultramafic rocks that occur within the felsic granulites. These were interpreted as fragments of upper mantle intercalated in the crustal rocks during subduction (Medaris *et al.*, 2006; Faryad, 2009). The UHP conditions of the felsic granulite were later confirmed by the discovery of micro-diamond and coesite inclusions in garnet and zircon (Perraki & Faryad, 2014). These findings concerning ultra-deep subduction of felsic rocks raise questions regarding the *P–T* trajectory during their exhumation and about the extent of granulite-facies re-equilibration of these rocks. According to Perraki & Faryad (2014), the micro-diamond and coesite in the felsic granulite were formed during subduction of crustal rocks to mantle depths and the granulite-facies overprint was a subsequent process that occurred after their exhumation to crustal levels (Faryad *et al.*, 2015).

This study is focused on the formation and preservation of major and trace element (primarily REE) zoning in garnet porphyroblasts from felsic granulites in the Kutná Hora Complex of the Bohemian Massif. In comparison with other granulite-facies rocks in the Moldanubian Zone, these felsic granulites show lower degrees of granulite-facies re-equilibration (Faryad *et al.*, 2010*b*). In addition to prograde zoning of major elements in garnet, the trace elements exhibit a complex core–rim distribution that is preserved as a result of the much slower diffusivities of Y + REE than for major divalent (Mg, Fe, Mn) cations (Hickmott & Schimizu, 1989; Lanzirotti, 1995; Chernoff & Carlson, 1999; Pyle & Spear, 1999). Such complex zoning could be interpreted as a result of major changes in *P–T–X* conditions or a polyphase metamorphic evolution. In the case of UHP rocks with subsequent granulite-facies metamorphism, the preservation of such zoning provides important information on the relative timing of geological processes under extreme *P–T* conditions. The zoning patterns of major and trace elements within garnet in combination with thermodynamic modeling allow us to estimate the different stages of the *P–T* path during UHP and subsequent granulite-facies metamorphism. The results of this work are used to discuss the main geotectonic processes during the Variscan Orogeny leading to the formation of HP–UHP rocks within the Bohemian Massif.

GEOLOGICAL SETTING

Metamorphic rocks in the Moldanubian Zone of the Bohemian Massif belong to three tectonic units, the Gföhl Unit and the Variegated and Monotonous Groups (Fig. 1a), which differ in terms of their lithologies and metamorphic conditions (Dawson & Carswell, 1990; Dallmeyer *et al.*, 1995; Medaris *et al.*, 1995). The Gföhl Unit contains granulite and migmatite, which exhibit generally higher metamorphic (granulite-facies) conditions compared with the Variegated and Monotonous Groups (amphibolite-facies conditions). All three units contain eclogite and peridotite, but garnet peridotite is known only from the Gföhl Unit, where it occurs within or adjacent to granulites and gneisses.

The high-grade metamorphic rocks of the Kutná Hora Complex are exposed in an ~50 km long NW–SE-oriented belt near the town of Kutná Hora, where they structurally overlie the medium-grade paragneiss sequence of the Monotonous Group (Fig. 1b). Based on its lithology and metamorphism, the Kutná Hora Complex has been correlated with the Gföhl Unit in the eastern part of the Moldanubian Zone (Synek & Oliveriová, 1993). It consists of two superimposed thrust sheets: at the top are granulites, granulite gneisses and migmatites with amphibolized and serpentinized mafic and ultramafic rocks and calc-silicates, whereas at the bottom are micaschists with lenses of amphibolite. The largest granulite body (the Běstvina granulite) consists mainly of felsic granulites, biotite gneisses and migmatites, additionally containing several small, isolated bodies of peridotite and eclogite (Pouba *et al.*, 1987; Synek & Oliveriová, 1993; Vrána *et al.*, 2005). It is exposed in the eastern part of the Kutná Hora Complex at the boundary with the Monotonous Group (Fig. 1c). The Monotonous Group beneath the Kutná Hora Complex is represented by partly migmatized kyanite/sillimanite + biotite ± muscovite ± cordierite paragneiss. At the contact with the micaschist zone, paragneiss from the Monotonous Group encloses several bodies of serpentinized peridotite, eclogite and garnet amphibolite (Synek & Oliveriová, 1993). Controversy exists about the pressure conditions of the Kutná Hora granulites. According to Vrána *et al.* (2005) and Nahodilová *et al.* (2014), the felsic granulites reached a maximum pressure of 2·3 GPa at 850–900°C. However, a UHP prograde *P–T* path and UHP conditions, similar to the hosted mafic and ultramafic bodies, were postulated by Faryad *et al.* (2010*b*).

The samples selected for this study come from the central part of the Běstvina granulite body where lenses of garnet peridotite with eclogite and garnet pyroxenite are exposed. They are from the same outcrop in which micro-diamond and coesite inclusions in garnet and zircon were identified (Perraki & Faryad, 2014). In contrast to other parts of the granulite body, which are characterized by light-colored banding parallel to a weak foliation, here the granulite has a mostly massive, medium-grained appearance.

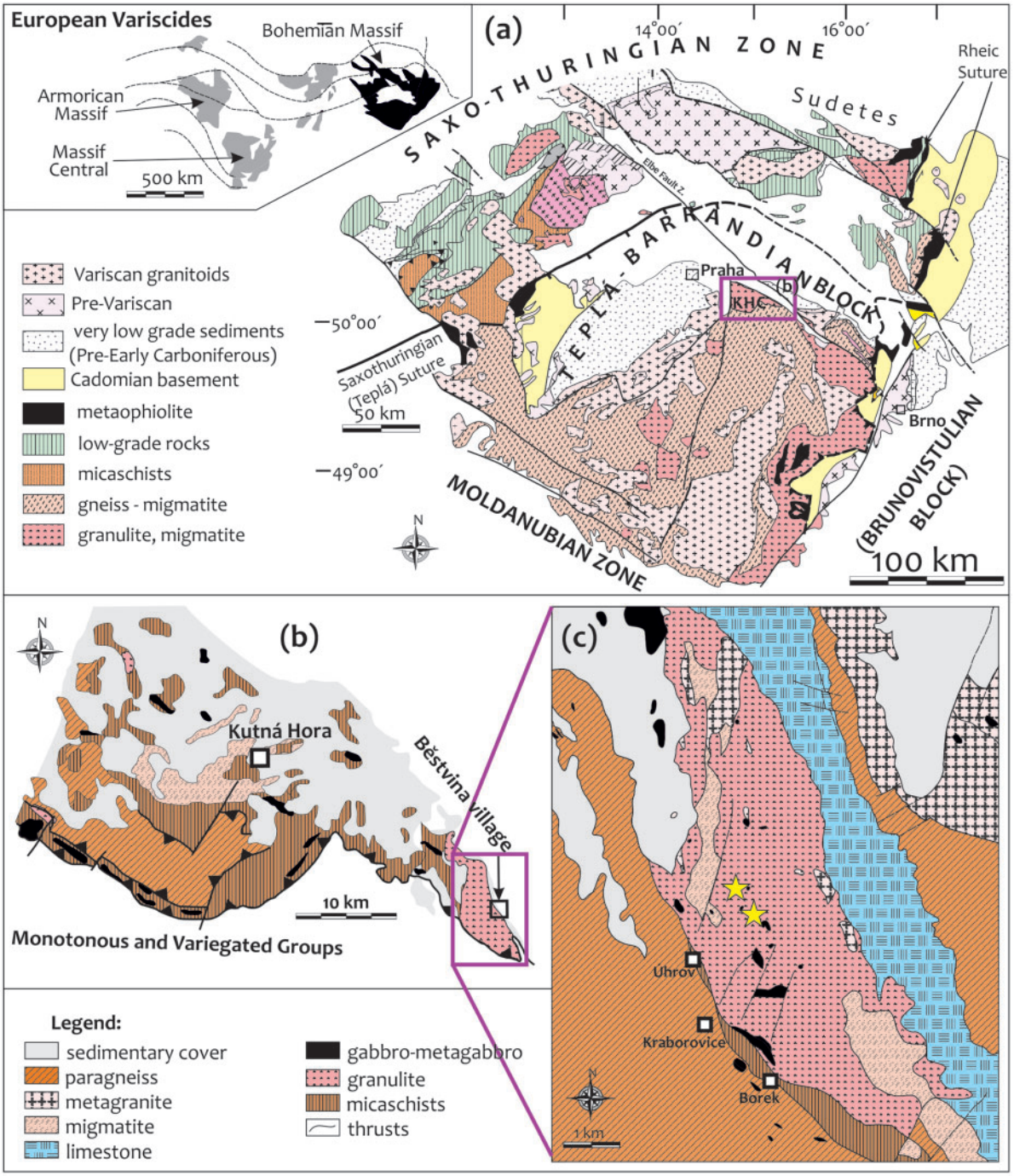

Fig. 1. (a) Simplified map of the Bohemian Massif after Franke (2000), Willner *et al.* (2002), Cháb *et al.* (2007) and Faryad & Kachlík, 2013; (b) map of the Kutná Hora Complex, simplified after Synek & Oliveriová (1993); (c) detail of the studied area of the Běstvina granulite, modified after Faryad *et al.* (2009). Stars indicate sample locations.

PETROGRAPHY AND TEXTURAL RELATIONS

The detailed petrography and textural relations of the Kutná Hora basement rocks, mainly of the Běstvina granulite body, have been discussed by Vrána *et al.* (2005), Faryad *et al.* (2010*b*) and Nahodilová *et al.* (2011). Two varieties of granulite are present. The most common is a fine- to medium-grained felsic variety with weak foliation highlighted by modal layering of 2–5 cm thick quartzo-feldspathic (leucocratic) layers alternating with garnet-rich (mesocratic) layers (Faryad *et al.*, 2009) (Fig. 2a). Rarely, they may contain lenses (about 3 m in size) of a dark, intermediate variety with porphyroblasts

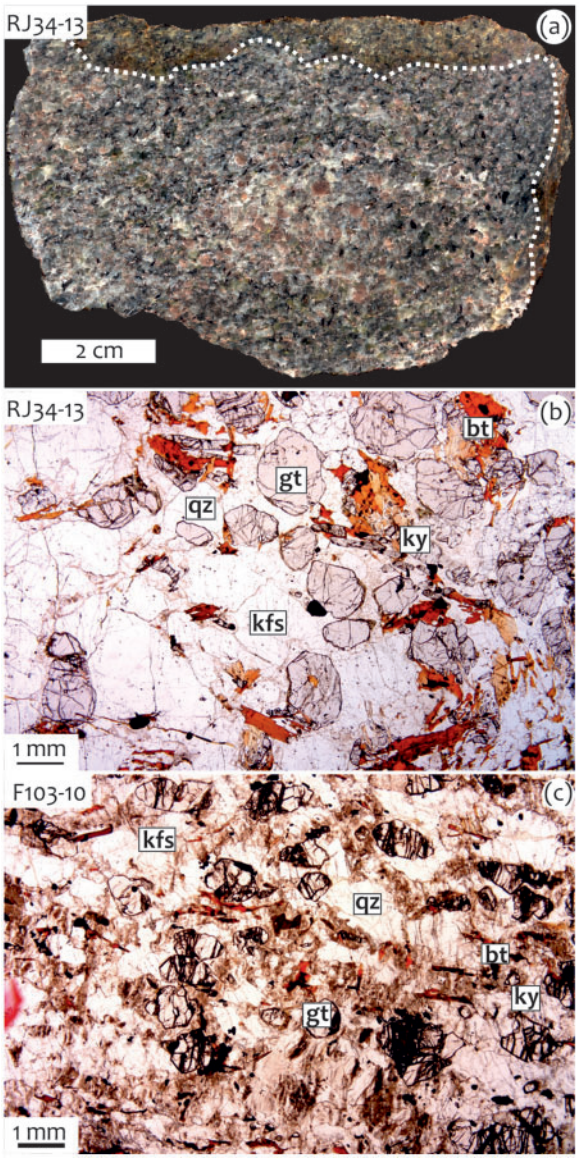

Fig. 2. (a) Hand-specimen photograph of a mesocratic layer of granulite with reddish garnet and dark biotite in a quartz + feldspar matrix; Běstvina granulite body (sample RJ34-13). Dotted line separates zone of weathering from the fresh part of the sample. (b) Photomicrograph of the mesocratic layer in RJ34-13. (c) Photomicrograph of the leucocratic layer F103-10. Abbreviations as in the main text.

of garnet in a weakly foliated or unfoliated matrix. The two varieties show continuous gradation into one other. The leucocratic layers in the felsic granulite are interpreted as the result of partial dehydration melting during granulite-facies metamorphism. The felsic granulite consists of ternary feldspar, quartz, garnet, kyanite, and rutile (Fig. 2b and c). Rarely, inclusions of Ti-phengite are found in garnet (Faryad *et al.*, 2010*b*). Compared with other felsic granulites in the Moldanubian Zone, kyanite is not replaced by sillimanite or spinel. The presence of biotite depends on the degree of retrogression and/or amphibolite-facies overprint.

The samples selected for this study come from the felsic variety of granulite with small amounts of biotite. They include both a mesocratic layer (Fig. 2a and b) with lower silica content (sample RJ34-13) and a leucocratic layer (sample F103-10, Fig. 2c) with higher silica content but lower CaO content. Sample F103-10 has a high content of quartz that occurs along thin layers with K-feldspar. Garnet and K-feldspar may form ~1 mm sized grains in the fine-grained matrix. Garnet usually contains inclusions of quartz, kyanite, K-feldspar, antiperthitic plagioclase, rutile and rarely phengite (Faryad *et al.*, 2010*b*). Some garnets have reaction coronas formed by biotite and plagioclase. Small garnet grains are partly chloritized. K-feldspar is usually perthitic (Fig. 3c) but antiperthitic feldspar is also present. Large kyanite grains are rimmed by plagioclase coronas and may contain inclusions of quartz. Apatite is a common accessory phase, which mostly occurs in the matrix at contacts with garnet grains (Fig. 3a) or rarely forms inclusions within garnet (Fig. 3b) or biotite. The apatite may contain exsolution lamellae of monazite. Separate monazite crystals can also be found in contact with apatite crystals (Fig. 3a). Polyphase inclusions (phengite + biotite) pseudomorphic after Ti-phengite were observed (Fig. 3d). Rare tabular-shaped graphite inclusions in garnet were also identified (Fig. 3e).

ANALYTICAL METHODS

Bulk-rock major and trace element concentrations were determined by wet chemical analysis and inductively coupled plasma-mass spectrometry (ICP-MS) using a Thermo X-Series II system, respectively, in the Geological Laboratory at Charles University in Prague. Trace elements were determined using a modified total digestion in mineral acids ($HF + HClO_4$) and borate fusion ($Na_2CO_3 + Na_2B_4O_7$) technique followed by conventional solution nebulization using a Thermo X-series II ICP-MS system. The ICP-MS analytical procedure and calibration have been described by Strnad *et al.* (2005). The analytical precision, calculated as one relative standard deviation (RSD), ranged from 0·5 to 5% for most elements. The QA/QC (quality assurance/quality control) was controlled using the AGV-2 and BCR-2 (USGS) reference materials.

Mineral analyses and compositional maps of major elements in garnet were determined by energy-dispersive X-ray analysis using a Vega Tescan scanning electron microscope at Charles University. Analytical conditions include an accelerating potential of 15 kV and a beam current of 800 pA.

For chemical analyses of minerals and variations of elements along garnet profiles a JEOL 6310 scanning electron microscope was used at the Institut für Erdwissenschaften, Karl-Franzens Universität, Graz, Austria, equipped with wavelength- and energy-dispersive spectrometers (WDS and EDS). Standards were garnet (Fe, Mg), adularia (K, Si, Al), rhodonite (Mn), jadeite (Na, WDS), and titanite (Ti, Ca). Sodium content was measured by WDS at conditions of 15 kV and 6 nA on PCD (probe current detector).

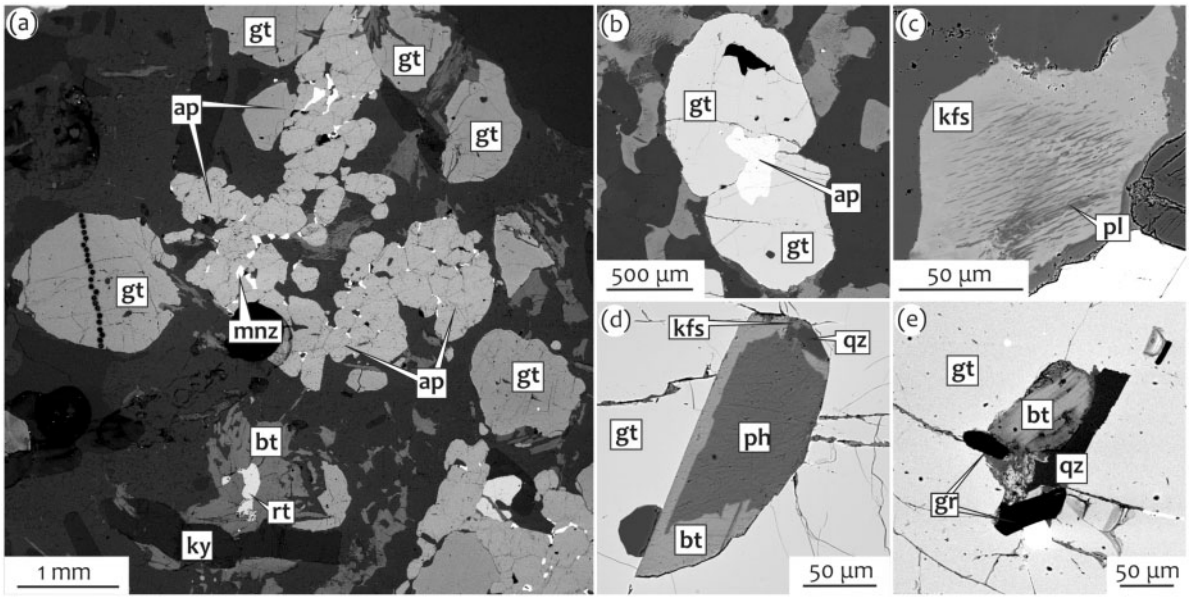

Fig. 3. Back-scattered electron images of felsic granulites. (a) Apatite with monazite in matrix (RJ34-13); (b) apatite between two garnet grains (F103-10); (c) perthitic feldspar in matrix (F103-10B); (d) polyphase inclusion after former Ti-rich phengite (F103-10); (e) graphite (gr) inclusions in garnet (F95-10).

Trace element and REE concentrations in garnet were analyzed with a laser ablation (LA)-ICP-MS system (ESI New Wave 193 nm LA system coupled with an Agilent 7500cx ICP-MS system) at the Central Laboratory for Water, Minerals and Rocks, NAWI Graz, Karl-Franzens-University Graz and Graz University of Technology, Austria. The material was ablated using a 193 nm laser pulsed at 8 Hz with a 35 μm spot size and energy of 6·5 J cm^{-2}. Helium was used as the carrier gas at a flow rate of 0·7 l min^{-1} and data were acquired in time-resolved mode. For each analysis a 30 s gas blank was obtained for background correction. The laser was active for 50 s followed by 45 s washout time. The NIST612 standard glass was routinely analyzed for standardization and to correct for drift, and standard NIST614 and USGS reference material BCR-2G were analyzed as unknowns to monitor the accuracy of the measurements. Counting statistics and reproducibility were usually better than 5% relative. However, taking uncertainties in reference material concentrations, elemental mass fractionation and instrumental drift into account, we estimate that the analytical uncertainty may be as much as 10% relative. Results from repeated NIST614 as well as BCR-2G measurements confirmed a reproducibility within ±10% of the reported values. Although the NIST612 reference material and the analyzed garnet contain a silicate-dominated matrix, some analytical uncertainties may arise from matrix effects. To test for matrix effects, the basaltic glass reference material BCR-2G, which contains a significantly different major element matrix, was analyzed. Because the obtained trace element and REE concentrations could be reproduced within the given uncertainties we concluded that matrix effects can be neglected. Data reduction was done using the Glitter software. For NIST612 the concentration values reported by Jochum *et al.* (2011) were used.

Additional microprobe analyses and X-ray maps of garnets were obtained on the JEOL JXA-8200 at the Eugen F. Stumpfl electron microprobe laboratory of the Universitätszentrum Angewandte Geowissenschaften (UZAG) Steiermark at Montanuniversität, Leoben. The conditions of operation were 15 kV with a 10 nA beam current for analyses and 150 nA for element mapping.

Element maps were also acquired on a Cameca SX100 electron microprobe in wavelength-dispersive mode at the Masaryk University in Brno, Czech Republic. Intensities of characteristic X-rays of Ca Kα, Ti Kα, P Kα, Cr Kα and Y Lα as well as one background for each line were collected at the following conditions: 20 kV, 200 nA, 1 μm beam diameter, 5–8 μm step (depending on the garnet size), and 0·8 s dwell time. The background intensities were subtracted from the characteristic X-ray intensities prior to graphic processing.

Mineral abbreviations in the text, figures and figure captions are those of Whitney & Evans (2010), except garnet, which is abbreviated as gt. Garnet end-members are $Alm = Fe^{2+}/(Fe^{2+} + Mg + Ca + Mn)$, $Grs = Ca/(Fe^{2+} + Mg + Ca + Mn)$, $Prp = Mg/(Fe^{2+} + Mg + Ca + Mn)$ and $Sps = Mn/(Fe^{2+} + Mg + Ca + Mn)$, and $X_{Fe} = Fe^{2+}/(Fe^{2+} + Mg)$.

BULK-ROCK COMPOSITIONS

Bulk-rock SiO_2 contents are 60·3 wt % (RJ34-13) and 71·6 wt % (F103-10). Sample F103-10 has lower Al_2O_3, FeO_t, MgO, CaO and TiO_2, but a higher K_2O content. Both samples have similar Na_2O contents (about 2 wt %) and MnO is below <0·12 wt %. Both of the samples were additionally analyzed for their trace element

Table 1: Whole-rock major and trace element compositions

Sample:	RJ34-13	F103-10		RJ34-13	F103-10
Chemical composition (wt % oxides)			*(ppm)*		
SiO_2	60·31	71·58	Rb	31·17	55·09
TiO_2	1·05	0·34	Sr	95·49	75·12
Al_2O_3	17·41	13·67	Y	53·30	5·2
Fe_2O_3	1·75	0·76	Zr	115·99	14·2
FeO	6·35	3·36	Nb	16·25	2·1
MnO	0·12	0·10	Ba	366·84	266·53
MgO	3·19	1·78	La	79·48	1·94
CaO	3·62	2·26	Ce	204·44	5·25
Na_2O	2·19	2·04	Pr	27·89	0·77
K_2O	1·34	4·06	Nd	117	3·95
P_2O_5	1·06	0·07	Sm	26·73	1·32
CO_2	0·60	0·40	Eu	3·67	0·26
Total	98·99	99·42	Gd	21·61	1·41
X_{Fe}	0·67	0·65	Tb	2·57	0·22
Modal proportion (%)			Dy	11·39	1·9
Qz	28	46	Ho	1·93	0·19
Fsp	42	31	Er	5·47	0·54
Gt	15	10	Tm	0·73	0·08
Bt	10	7	Yb	4·87	0·55
Ky	3	3	Lu	0·7	0·07
Accessory phases	2	3	Hf	3·78	0·54
			Pb	29·16	0·19
			Th	4·79	<0·25
			U	2·27	0·04

chemistry, the mesocratic sample recording higher concentrations of REE than the leucocratic sample (Table 1).

COMPOSITIONAL ZONING IN GARNET

Major elements

Garnets from both the mesocratic and leucocratic layers of the felsic granulite show strong compositional zoning, differing from each other in terms of grossular and almandine contents [$Grs_{9–20}$ $Alm_{49–257}$ $Prp_{29–236}$ $Sps_{0–21}$ (sample RJ34-13) and $Grs_{18–234}$ $Alm_{39–246}$ $Prp_{16–238}$ $Sps_{1–22}$ (F103-10)]. Although the bulk-rock composition of the mesocratic layer (RJ34-13) shows higher values of all four oxides (FeO, MgO, CaO, MnO; Table 1), the differing garnet compositions reflect the lower value of $X_{Ca} = Ca/(Ca + Fe^{2+} + Mg + Mn) = 0·27$ and higher $X_{Fe} = 0·48$ in this sample compared with that in the leucocratic layer ($X_{Ca} = 0·30$, $X_{Fe} = 0·45$). Clear prograde garnet zoning is documented by the higher spessartine content in the core of the garnet from the leucocratic sample (Fig. 4d and f). The pyrope, grossular and almandine zoning patterns are complex with at least two segments, which correspond to the core and mantle–rim sections (see below).

In sample RJ34-13 (Fig. 4a and b), grossular content decreases from the core (Grs = 20 mol %) towards the rim, with a weak annular minimum (17 mol %) followed by an increase to 18 mol % and finally a significant decrease at the rim. The pyrope content shows an opposite trend with a less variable compositional profile than grossular. The lowest pyrope value (29 mol %) is recorded in the core with a slight increase (the first maximum at 31 mol %) and then a decrease that is followed by another increase at the rim of the grain. Almandine content has a similar trend to pyrope. The almandine content is lowest in the core (49 mol %) and increases towards the rim. Spessartine content is low and reveals no zonation from core to rim.

Two grains from sample F103-10 (Fig. 4c and e) show similar Ca distribution to that in sample RJ34-13, but with more pronounced zonation. Strong compositional zoning occurs in the larger grain (Fig. 4f) with maximum grossular content of 34 mol % in the core and about 20 mol % in the rim. The rimward decrease in grossular is asymmetrical; it is steep on the left side but relatively flat on the right side, where it shows a slight increase at the rim. Spessartine and almandine also show a rimward decrease; a slight increase in spessartine at the rim may indicate back-diffusion owing to garnet consumption (Chakraborty & Ganguly, 1992; Kohn & Spear, 2000). Variations in all three constituents are compensated for by pyrope, which has the lowest value of 16 mol % in the core and contents reaching about 39 mol % at the rim. In addition to relatively weaker zoning, the garnet grain in Fig. 4d differs from that in Fig. 4f by comparatively lower grossular and spessartine and higher pyrope contents in the core.

Trace elements

To compare the major and trace element zoning in garnet, analyses were obtained along the same garnet profiles from samples RJ34-13 and F103-10 (Figs 4–6 and Supplementary Data, Table 1S; supplementary data are available for downloading at http://www.petrology.oxfordjournals.org). Garnets from both samples display core to rim zonation of Y, Ti, Cr, V and of heavy REE (HREE; Er, Tm, Yb, Lu), middle REE (MREE; Gd, Tb, Dy, Ho) and light REE (LREE; Nd, Sm, Eu) (Figs 5 and 6). Yttrium and most REE show two maxima, the first in the core section (segment I), which is probably related to nucleation of garnet, and the second in the mantle–rim section (segment II), suggesting a dramatic change in *P–T–X* conditions during garnet crystallization.

Garnet from sample RJ34-13 shows a bell-shaped distribution of Y, HREE, MREE and LREE contents (Fig. 5). Ti shows a high concentration in the core with a decrease towards the border of the core part and second maxima and a subsequent decrease towards the rim (Fig. 5b and f). Vanadium does not show clear zoning at the boundaries of segments I and II, but it generally increases towards the rim (Fig. 5h). The most pronounced zoning is in Y + HREE. After a decrease to a local minimum, all elements start to increase again and reach a second maximum. The second maximum actually shows higher values than in the core of the garnet crystal. The final part of the distribution profile is characterized by a decrease of all elements towards the rim of garnet. Some MREE (Gd, Tb, Dy) show a slight increase at the outermost rim of the garnet (Fig. 5m–o).

Phosphorus content reveals multiple zoning features (Fig. 5d). In addition to high P contents along the rim of

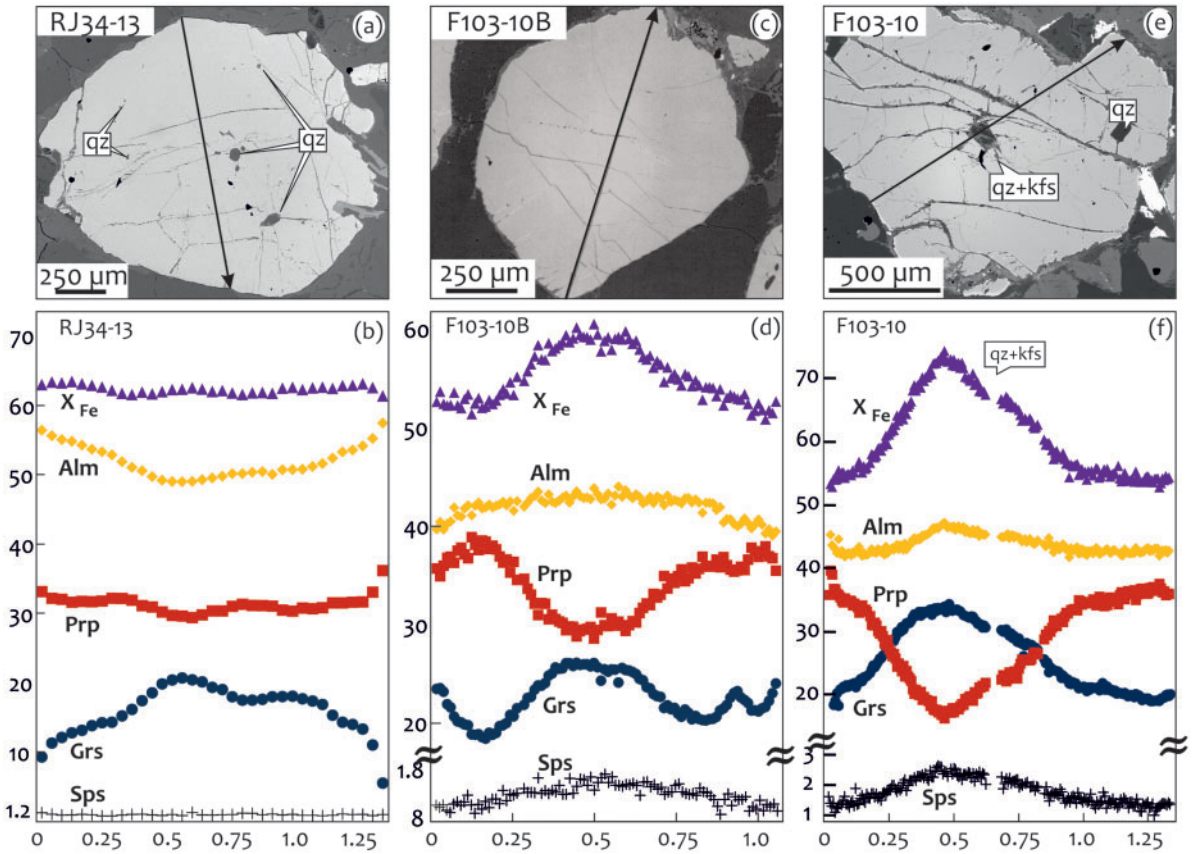

Fig. 4. Back-scattered electron images and major element profiles (rim–core–rim) of selected garnets from mesocratic granulite RJ34-13 (a, b) and leucocratic granulite F103-10 (c–f). *y*-axes indicate molar per cent; *x*-axes of profiles are rim–core–rim distances in millimetres.

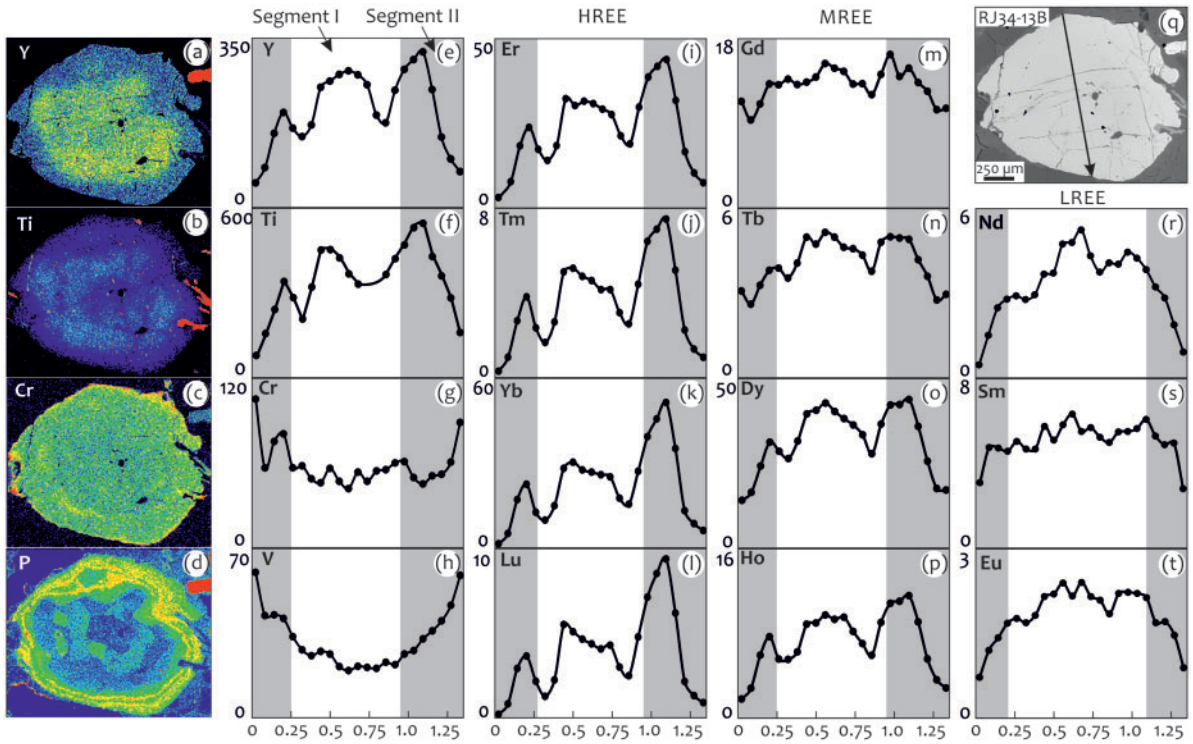

Fig. 5. Garnet from mesocratic layer in granulite RJ34-13; trace element compositional maps of Y, Ti, Cr, P (a–d) and trace element profiles (e–t). Segments I and II refer to HP–UHP and granulite-facies garnet, respectively (for details see text).

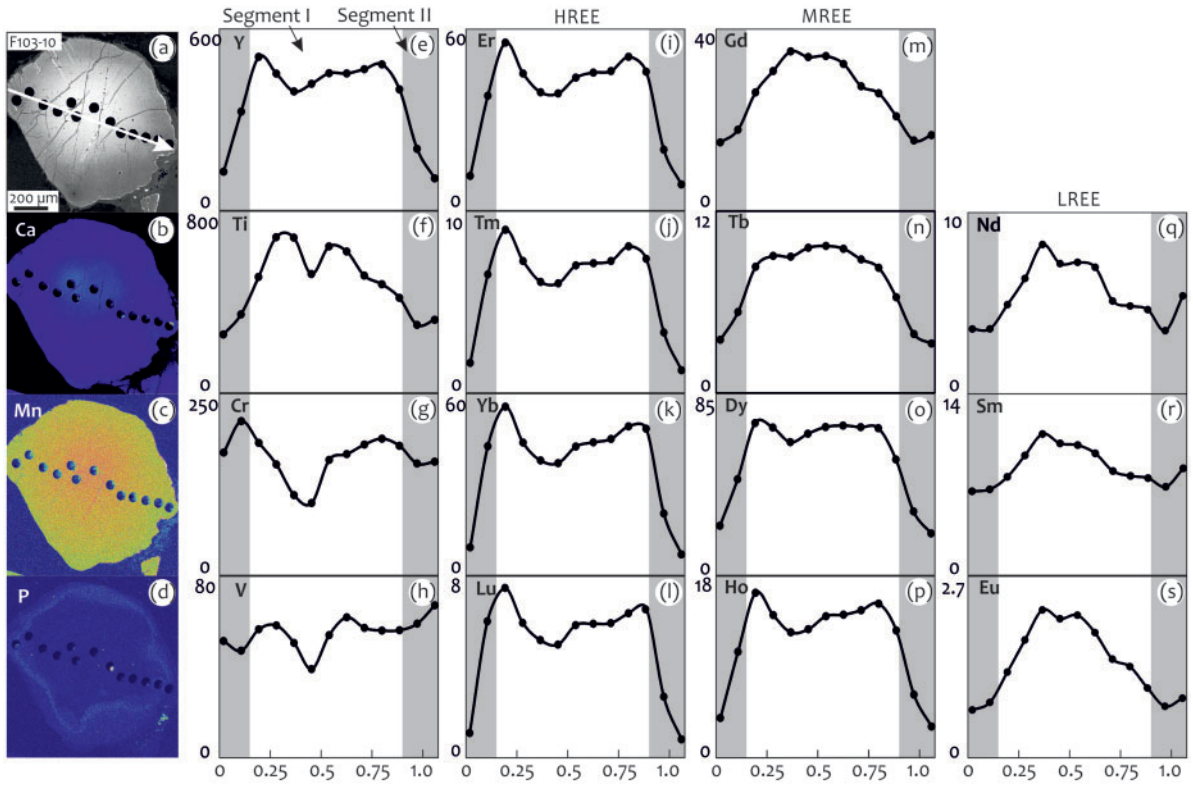

Fig. 6. Garnet from leucocratic layer in granulite F103-10; back-scattered electron image (a), compositional maps of Ca, Mn and P (b–d) and trace element profiles (e–s). Segments I and II are as in Fig. 5.

the garnet (ring shape), concentric zoning with slightly elevated P content is present in the core. In contrast to the irregular shape of the ring, the core zoning seems to follow the crystallographic planes of the garnet. Three patchy domains with a relatively high P content can also be observed in the mantle part of the garnet grain.

Trace element zoning patterns in sample F103-10 are similar to those in RJ34-10, but the central peak is not clearly visible. However, the second peak of Y + HREE is clear (Fig. 6). Y, Ti, Cr and V increase from the core to the annular maxima. Ti and V reach this point closer to the core (Fig. 6f and g). From the annular maxima, values for all these elements (except vanadium) decrease towards the rim of the garnet. HREE and the heaviest of the MREE (Dy, Ho) increase from the core to the annular maxima. Gd, Tb and LREE have maxima at the garnet core and decrease continuously towards the rim. After reaching the annular maxima, most elements show a significant drop towards the rim. P concentration is low in the garnet core, but high at the outermost rim (Fig. 6d).

PRESSURE–TEMPERATURE CALCULATIONS

To constrain the *P–T* path for the Kutná Hora felsic granulites, the following points need to be considered: (1) the rocks preserve garnet with prograde zoning; (2) they experienced UHP conditions in the coesite and micro-diamond stability fields (Perraki & Faryad, 2014); (3) they passed through a granulite-facies overprint at about 850–900°C (Nahodilová *et al.*, 2011). Therefore pseudosection modeling combined with conventional thermobarometry was used to estimate the *P–T* conditions and trajectory for the HP–UHP event and subsequent granulite-facies overprint. It should be noted that a number of uncertainties in the estimated *P–T* conditions are associated with this approach, owing to the absence of precisely determined thermodynamic data for minerals at such high temperature and pressure conditions and possible modification of garnet composition. However, this approach helps to trace the possible *P–T* path during the prograde stage of garnet formation and during the granulite-facies overprint.

Pseudosection modeling

The pseudosection method was used to decipher the changes in the mineral assemblage and modal volume of garnet in the *P–T* ranges 400–800°C and 0·4–4 GPa, and 600–1000°C and 0·5–2·5 GPa, respectively (Figs 7 and 8). The calculation was performed in the system SiO_2–TiO_2–Al_2O_3–FeO–MgO–CaO–MnO–Na_2O–K_2O–H_2O (KNMnCFMASHT) by Gibbs energy minimization using the computer program Perple_X 6.6.8 (Connolly, 2005) with the internally consistent thermodynamic dataset for mineral end-members and aqueous fluids of Holland & Powell (1998), upgraded in 2004. The following non-ideal solution models were used: garnet (Holland & Powell, 1998), phengite (Coggon & Holland, 2002), biotite (Powell & Holland, 1999), plagioclase

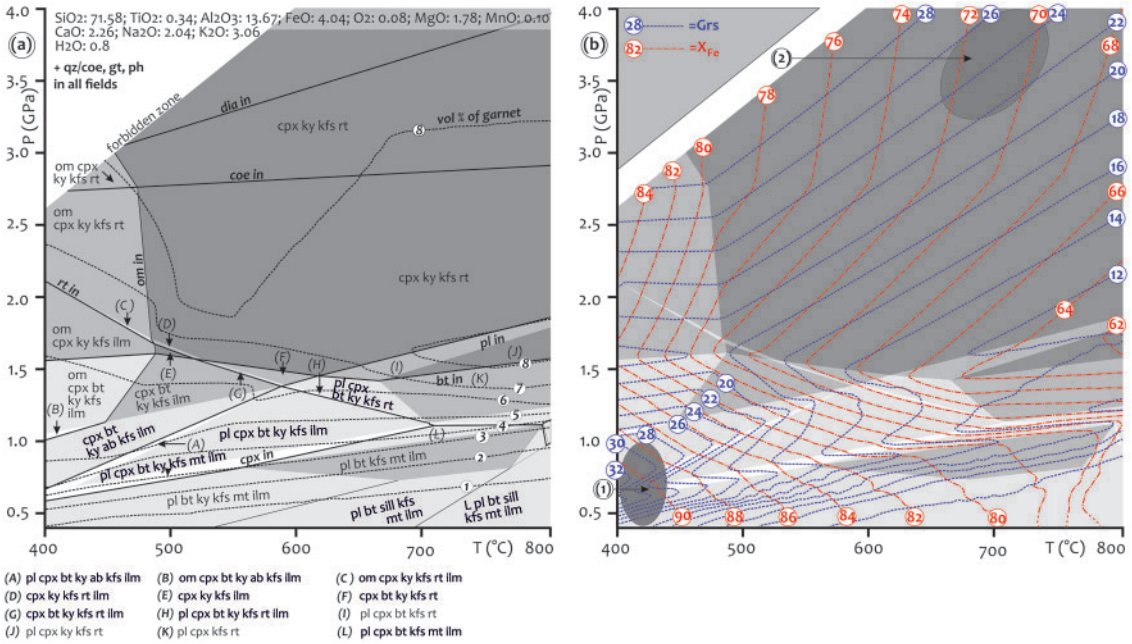

Fig. 7. Low-temperature *P–T* pseudosection for a felsic layer in the Kutná Hora granulite (F103-10): (a) shows fields of stable mineral assemblage; (b) shows grossular and X_{Fe} isopleths. In (a) bold lines show in-reactions of index minerals, and dotted lines indicate modal volume per cent of garnet. Labels for small *P–T* fields are omitted for clarity.

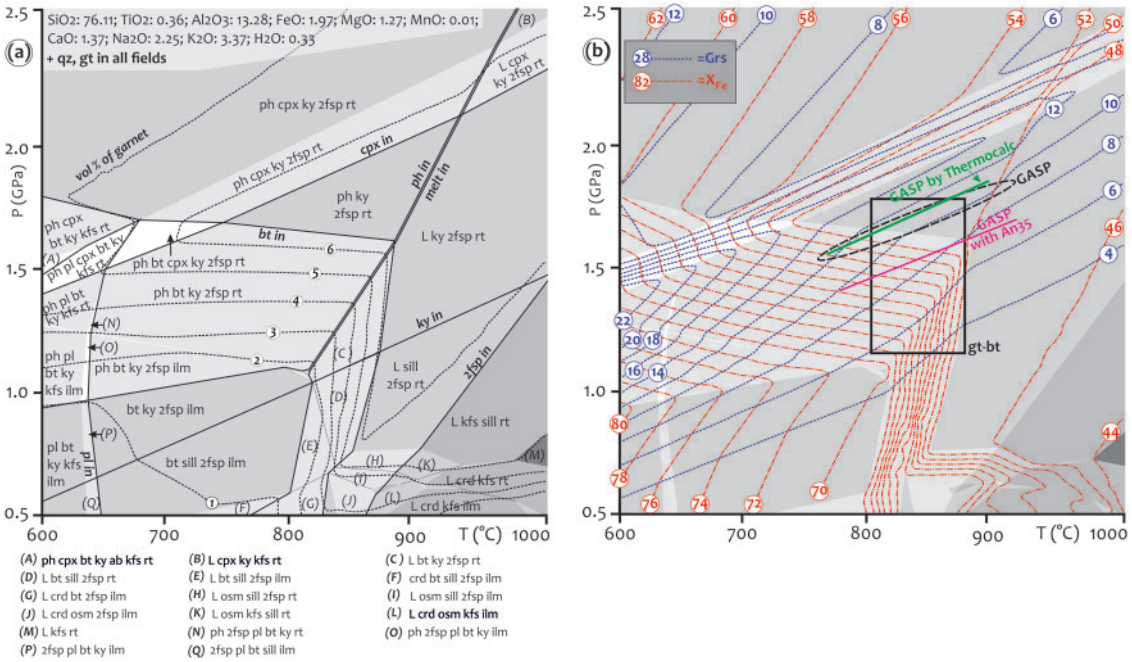

Fig. 8. High-temperature *P–T* pseudosection for a felsic layer in the Kutná Hora granulite (F103-10). (a) shows fields of stable mineral assemblages. Labels for small *P–T* fields are omitted for clarity. Bold lines show in-reactions of index minerals; dotted lines indicate modal volume per cent of garnet. (b) shows grossular and X_{Fe} isopleths. Bold rectangle and dashed ellipse indicate the temperature range based on garnet–biotite thermometry [calibrations of Bhattacharya *et al.* (1992) and Holdaway (2000)] and GASP barometry [calibrations of Hodges & Spear (1982) and Ganguly & Saxena (1984)], respectively (Table 2). Bold lines show pressures obtained by GASP barometry with plagioclase composition An_{35} calculated from the pseudosection and GASP barometry using THERMOCALC, respectively.

(Newton *et al.*, 1980), feldspar (Benisek *et al.*, 2010), omphacite (Holland & Powell, 1996), clinopyroxene (Holland & Powell, 1996), chlorite (Holland *et al.*, 1998) and melt (Holland & Powell, 2001). The effect of ferric iron was explored by adding oxygen as an additional component to the system. Addition of up to 0·08 wt % O_2 leads to the stability of magnetite, but has no significant effects on omphacite, garnet or biotite equilibria.

Considering granite as a potential source material for transformation into felsic granulite (Janoušek *et al.*, 2004), an initial water content of about 0·8 wt % for the low-temperature part of the pseudosection was selected. This water content was calculated based on the approximate mica content in granite [following the method adapted from Proyer (2003)]. To analyze possible *P–T* conditions for the formation of the garnet core, sample F103-10 with pronounced compositional zoning and a high grossular content in garnet was chosen. Because of its slow diffusion coefficients, Ca has a significant effect in preventing the overall compositional modification of garnet through multicomponent diffusion with other divalent cations (Chakraborty & Ganguly, 1992). This is demonstrated by the preserved bell-shaped Mn (Sps) distribution in the garnet core (Fig. 4f). Figure 7a shows the calculated pseudosection, where garnet is stable in all fields in the selected *P–T* range. Except for sodic clinopyroxene, all phases (including phengite as inclusions in garnet) were observed in the rock. The lack of sodic clinopyroxene in HP felsic granulites was discussed by Faryad *et al.* (2010*b*). Based on phase relations in felsic granulite and inclusion patterns in garnet, Faryad *et al.* showed that breakdown of sodic clinopyroxene, which was once in equilibrium with the host Ca-rich garnet, must have occurred relatively early in favor of sodic plagioclase. In contrast, in intermediate rocks the transition to a plagioclase-bearing assemblage occurs at lower pressures, and in very Ca-rich protoliths diopside-rich clinopyroxene coexists with calcic plagioclase and Ca-depleted garnet.

Based on the calculated volume isopleths of garnet in sample F103-10, most garnet (about 5–6 vol. %) was formed below 1 GPa and a subsequent increase to 9 vol. % occurred in the coesite stability field above 3 GPa (Fig. 7a). The high grossular content (34 mol %), measured in the garnet core of sample F103-10 (Fig. 4f), is near the maximum value (36 mol %, Fig. 7b) that was modelled for this sample. This suggests garnet nucleation at a temperature of about 400°C and pressure of 0·4 GPa [field (1) in Fig. 7b]. Based on the compositional isopleths in garnet, the grossular content in the garnet core was not strongly modified. On the other hand, the corresponding X_{Fe} values for the core were changed by almost 20% from 91% (based on the pseudosection, Fig. 7b) to 73% (measured value in Fig. 4f) in the same field (1). If we consider that the composition profiles of garnet at the interface between core and mantle–rim parts signify the UHP stage, the grossular isopleth with 22–25 mol % (Fig. 4f) yields temperatures of 650–750°C in the coesite or even diamond stability field [field (2) in Fig. 7b]. The corresponding X_{Fe} value of about 55–57% in the measured profile (Fig. 4f) and 70–72% in the calculated isopleths means about 20% decrease of X_{Fe} owing to diffusion. However, as the rocks reached the diamond stability field, the measured grossular content should be modified through diffusion by at least 2–3 mol % at the interface between core and mantle–rim parts of the garnet (Fig. 7a).

Figure 8a shows the pseudosection calculated for the granulite-facies stage (sample F103-10). A water content of 0·33 wt % was determined for the high-temperature stage based on maximum modal content of biotite (up to 5%) in well-preserved (non-retrogressed) samples. The low water content is due to metamorphic dehydration reactions during temperature increase. However, there is some uncertainty in the calculation of *P–T* conditions for the granulite-facies event, as some material is isolated within already crystallized garnet during the HP stage and does not participate in the subsequent metamorphic reactions. Therefore, the core composition of garnet (segment I in Fig. 6) was subtracted from the bulk-rock composition in sample F103-10. The effective bulk composition, used for the pseudosection in Fig. 8a, was calculated by integration of the mineral mode (segment I in Fig. 6) and contents of each element in the microprobe analyses (Stüwe, 1997; Konrad-Schmolke *et al.*, 2008*a*).

The garnet volume isopleths indicate that most garnet was formed during heating from 800°C upwards or during a pressure increase above 1 GPa. Assuming that the granulite-facies event occurred after exhumation of the rocks to lower to middle crustal levels, about 5 vol. % of garnet should have formed in sample F103-10 during the granulite-facies stage at 850–900°C, as estimated based on thermobarometric calculations for granulites from this locality (Nahodilová *et al.*, 2011, 2014). However, the grossular content of 16–20 mol % in the mantle part of garnet (Fig. 4d and f) indicates a temperature of about 700°C (Fig. 8b). Further increase of temperature is documented by a decrease of X_{Fe} and Grs (Fig. 4f). The slight increase of Ca and decrease of Mg in the outer rim of garnet (Fig. 4f) could be due to diffusion modification during cooling, as can be postulated from the back-diffusion of manganese.

With increasing temperature, dehydration of phengitic muscovite occurs and melt is produced (Fig. 8a and b). At low pressures, kyanite transforms to sillimanite and rutile changes to ilmenite. Radical change in the chemistry of garnet occurs during temperature increase and pressure decrease owing to the breakdown of pyroxene and creation of plagioclase at the expense of garnet. At high temperatures, only limited amounts of garnet are formed, but significant modification of elemental concentrations occurs at the outermost edge of the garnet crystals in a short time interval (Faryad & Chakraborty, 2005). During cooling and retrogression, newly formed biotite has a significant influence on magnesium and iron diffusion in garnet.

Conventional thermobarometry

Except for kyanite, garnet cores and rutile, all the minerals formed during the HP–UHP event underwent recrystallization during the granulite-facies overprint. Therefore, biotite, plagioclase and garnet rims were used to estimate the *P–T* conditions for the granulite-facies event. Based on the pseudosection modeling

(Fig. 8a), biotite forms during cooling at about 850°C. Plagioclase is stable and based on the pseudosection calculations a ternary Na–Ca plagioclase with composition of An_{35} can be stable at 850–900°C and 1·5–1·8 GPa. However, most analyzed plagioclase in the matrix of the studied samples is $An_{22–23}$. The lower anorthite content, consistent with the increase of Grs and decrease of Prp and X_{Fe} at garnet rims (Fig. 4d), suggests that garnet was partly formed during cooling. The garnet–biotite thermometer, used for the high-Mg and low-Ca rim in sample F103-10, yields temperatures in the range 750–900°C (Table 2). The lowest temperature of 744 ± 29°C was obtained using the calibration of Perchuk & Lavrenťeva (1983) and the highest temperature of 907 ± 83°C by using that of Dasgupta *et al.* (1991). Temperatures calculated using Bhattacharya *et al.* (1992) and Holdaway (2000) are close to the biotite-in boundary obtained from the pseudosection modeling. GASP barometry used for the analyzed plagioclase (An_{22}) and garnet with the lowest Ca content yielded pressures of 1·6–1·7 GPa at 850°C. Lower pressures of 1·4–1·5 GPa can be obtained using a plagioclase composition (An_{35}) based on the pseudosection calculation. Similar temperatures of 850°C and pressures of 1·76 ± 0·02 GPa (Table 2) were obtained by calculation of average *P–T* using the THERMOCALC 3.37 package (Powell *et al.*, 1998; most recent upgrade) and the thermodynamic dataset 5.5 (Holland & Powell, 1998).

Table 2: Representative mineral analyses used for conventional thermobarometry

Sample:	F103-10					
Mineral:	gt1	gt2	gt3	bt1	bt2	pl
SiO_2 (wt %)	39·05	39·08	39·15	38·66	37·64	62·64
TiO_2	0·07	0·03	0·05	4·93	4·95	0·01
Al_2O_3	22·72	21·85	21·89	17·31	15·18	23·16
FeO	19·70	20·50	21·14	8·68	10·47	—
MnO	0·54	0·60	0·70	0·06	0·05	—
MgO	10·45	9·72	10·27	15·81	15·34	—
CaO	7·05	7·10	6·52	0·08	0·07	4·65
Na_2O	—	0·03	0·06	0·19	0·09	9·05
K_2O	0·03	—	0·02	9·90	9·69	0·08
Total	99·58	98·91	99·80	95·86	94·51	99·47
Si (per ox.)	2·95	2·99	2·96	2·90	2·90	2·78
Ti	0·003	0·001	0·003	0·28	0·28	—
Al	2·02	1·96	1·95	1·52	1·38	1·21
Fe	1·17	1·25	1·21	0·54	0·68	—
Mn	0·03	0·04	0·04	0·003	0·003	—
Mg	1·18	1·11	1·16	1·77	1·76	—
Ca	0·57	0·58	0·52	0·006	0·006	0·22
Na	—	—	—	0·03	0·01	078
K	—	—	—	0·95	0·95	—

	Temperature calculated at 1·4 GPa (°C)						
	gt1–bt1	gt2–bt1	gt3–bt1	gt1–bt2	gt2–bt2	gt3–bt2	Average
B92	783	745	761	858	811	832	798 ± 50
Dasg91	865	807	832	1003	949	983	906 ± 88
PL83	728	715	716	785	751	771	744 ± 31
H2000	923	823	881	923	823	881	875 ± 45

	Pressure calculated at 850°C (GPa)						
	gt1–bt1	gt2–bt1	gt3–bt1	gt1–bt2	gt2–bt2	gt3–bt2	Average
HS82	1·6	1·6	1·57	1·6	1·6	1·57	1·59 ± 0·02
GS84	1·79	1·78	1·76	1·79	1·78	1·76	1·78 ± 0·02
HC85	1·72	1·73	1·69	1·73	1·73	1·69	1·72 ± 0·02
K89	1·78	1·79	1·75	1·78	1·79	1·75	1·77 ± 0·02
T_{calc}	1·78	1·77	1·73	1·78	1·77	1·73	1·76 ± 0·02

B92, Bhattacharya *et al.* (1992); Dasg91, Dasgupta *et al.* (1991); PL83, Perchuk & Lavrent'eva (1983); H2000, Holdaway (2000); HS82, Hodges & Spear (1982); GS84, Ganguly & Saxena (1984); HC85, Hodges & Crowley (1985); K89, Koziol (1989); T_{calc}, THERMOCALC (Powell *et al.*, 1998).

DISCUSSION

In addition to major element zoning in garnet from such high-grade rocks, the striking feature of these samples is the presence of two annular trace element and REE maxima in garnet porphyroblasts. To assess or reconstruct the early *P–T* history of the rocks, we first need to discuss the trace element behavior in garnet during high-grade metamorphism and discuss the possible origins of the annular maxima seen in the garnets.

Origin of the annular maxima of Y + REE in the granulite-facies garnet

As indicated by Pyle & Spear (1999), the trace element distribution recorded by any metamorphic rock is a result of the reaction history of the entire rock. Each unique reaction reflects the modal contents of the major phases involved in the reaction. However, also important is the presence of trace element-bearing accessory phases, which buffer trace element activities and can exert very strong trace element partitioning controls. Incorporation of Y + REE into natural garnet is mostly assumed to be by menzerite-like or alkali substitutions with relatively low energetic cost (Carlson *et al.*, 2014). The energetic costs decrease significantly as the host-garnet unit-cell dimension expands, decrease very modestly as temperature rises or pressure falls, and decrease substantially with the contraction in ionic radius across the lanthanide series. When studying the origin of compositional zoning in garnet numerous factors controlling the distribution of major and trace elements should be considered (Lanzirotti, 1995; Schwandt *et al.*, 1996). These include the following: (1) element fractionation during mineral growth (e.g. Hollister, 1966; Cygan & Lasaga, 1982; Hickmott *et al.*, 1987); (2) slow re-equilibration of cations by intracrystalline (volume) diffusion (e.g. Anderson & Buckley, 1973; Chakraborty & Ganguly, 1992; Carlson, 2012); (3) limitations of intergranular diffusion of cations at the mineral–matrix interface (e.g. Carlson, 1989); (4) interaction with a metasomatic fluid (e.g. Hickmott *et al.*, 1987; Chamberlain & Conrad, 1993; Erambert & Austrheim, 1993; Jamtveit *et al.*, 1993; Young & Rumble, 1993); (5) the breakdown or growth of trace element-rich minerals (Hickmott & Spear, 1992; Chernoff & Carlson, 1999).

In addition to the classic bell-shaped zoning patterns, which are considered to occur as a result of a fractionation–depletion mechanism during garnet growth (e.g. Hollister, 1966; Tracy *et al.*, 1976; Tracy,

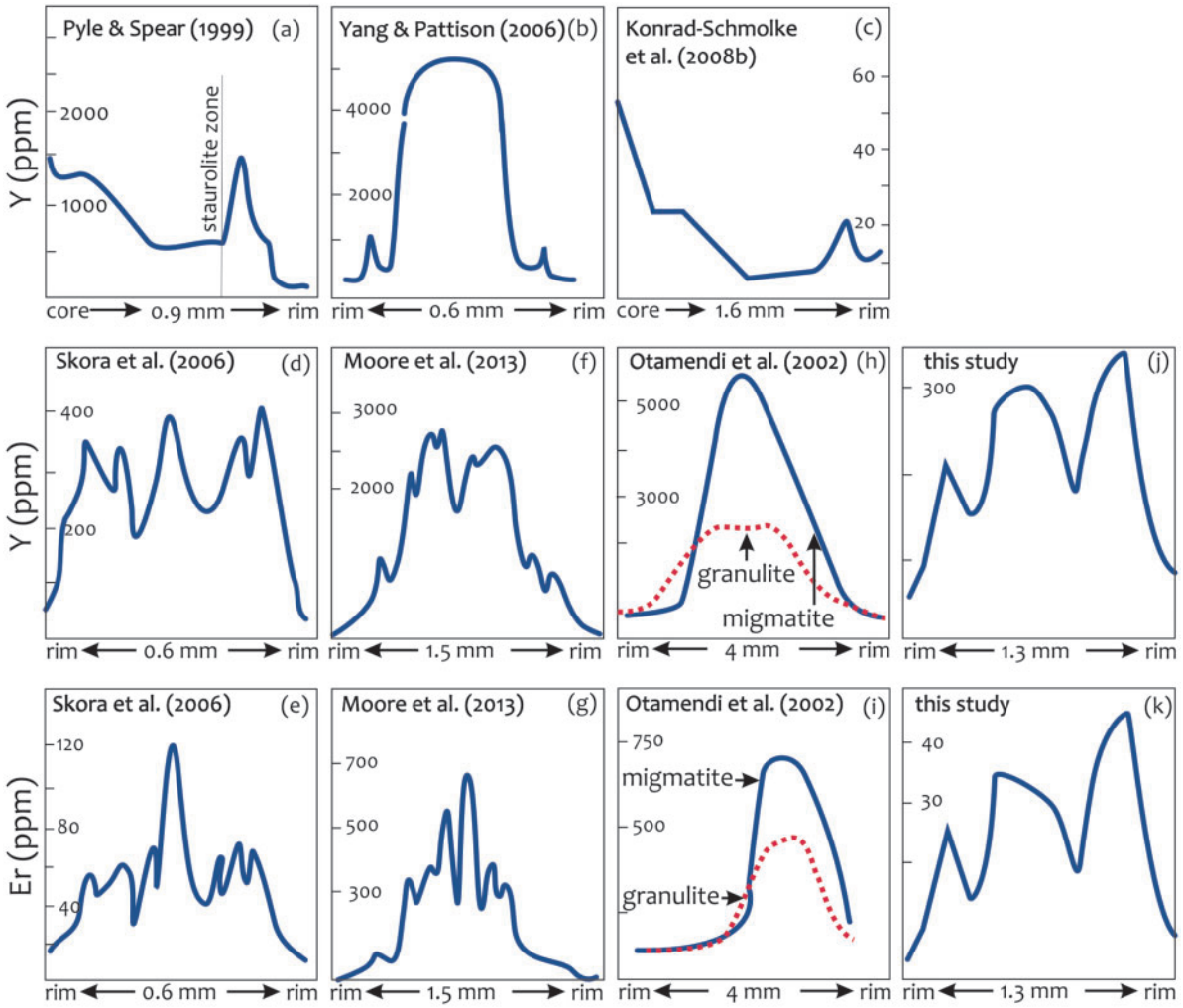

Fig. 9. Summary of distribution of Y + REE and annular peaks in garnet from various metamorphic terranes as discussed in the text. (a) Staurolite-grade metapelite (British Columbia); (b) staurolite schist (South Dakota); (c) eclogite (Gneiss Complex, Norway); (d, e) eclogite (Zermatt–Saas Zone); (f, g) metapelite (Picuris Mountains); (h, i) migmatite and granulite (Sierra de Pampeanas, Argentina); (j, k) felsic granulite (the Kutná Hora Complex, Bohemian Massif). Data sources are as indicated.

1982), the annular peak of Y and HREE near the rim of garnet crystals can be explained in various ways (Fig. 9). Pyle & Spear (1999) investigated metapelitic rocks in garnet, staurolite, sillimanite and migmatite zones, where they observed high-Y annuli near garnet rims. Those researchers interpreted this high-Y peak as the result of partial garnet consumption in the staurolite zone (Fig. 9a), where Y released into the matrix was incorporated back into garnet during its second stage of growth. Similarly, an annular peak in Y was reported by Yang & Pattison (2006) from pelitic rocks metamorphosed in the garnet to sillimanite zone. The rocks are rich in monazite, and Yang & Pattison found an Y peak in garnet below the staurolite zone (Fig. 9b). Based on monazite geochronology those workers concluded that the annular maximum was the result of decomposition of accessory phases rich in Y and REE. Konrad-Schmolke *et al.* (2008*b*) explained an annular peak of REE, observed in garnet from UHP eclogite, by changes in mineral assemblage and fractionation of REE during garnet formation (Fig. 9c). Using pseudosection modeling those workers calculated the modal proportion of minerals along the high-pressure *P–T* trajectory and interpreted the annular peak, similar to that in calcareous pelites (Hickmott & Spear, 1992), to reflect discontinuous breakdown of zoisite. Therefore, mineral reactions, including resorption of previously crystallized garnet, can liberate REE or change their bulk partition coefficients, and are important for understanding trace element distribution in garnet (e.g. Hickmott *et al.*, 1987; Spear & Kohn, 1996).

A different mechanism for the Y + REE annuli formation in garnets from UHP eclogites was proposed by Skora *et al.* (2006). According to those researchers, the peak is due to uptake of REE limited by rates of intergranular diffusion during garnet growth (Fig. 9d and e). This occurs when faster diffusion relaxes the concentration gradient in the intergranular medium of the matrix, which allows the garnet to incorporate greater concentrations of the REE when higher temperatures are

reached. This model was later adapted by Moore *et al.* (2013), who studied REE distributions in garnet with annular peaks from quartz pelitic schists and gneisses (Fig. 9f and g). However, a study by Otamendi *et al.* (2002) indicated that garnet with strong peaks of Y and HREE in the core without any annuli near the rims can be present in granulite-facies rocks (Fig. 9h and i). As shown by Cheng *et al.* (2007) and Faryad *et al.* (2010*a*), annular peak of REE as well as of manganese contents can occur during atoll garnet formation. The early formed small garnet grains or the cores of large crystals can be dissolved owing to their instability at higher *P–T* conditions. The elements released from the core are transported to the matrix by fluid infiltration through fractures and stabilize new garnet, which continuously overgrows the older crystal. In addition, a patchy and unsystematic distribution of REE, with irregular fluctuations at scales of a few tens of micrometres, can occur in garnet as a result of former accessory phases or pre-existing heterogeneities in the matrix during crystal growth (e.g. Yang & Rivers, 2002; Hirsch *et al.*, 2003).

In all of the above-mentioned models, a single metamorphic event is considered for garnet formation. In a polymetamorphic terrane, garnet can be partially replaced during exhumation or cooling and the elements released into the matrix will raise the activity of Y and REE in the environment. This is the case for the Moldanubian Zone granulites, for which two separate metamorphic events are assumed (Faryad & Fišera, 2015; Faryad *et al.*, 2015). The first of these events is the HP–UHP event and the second is the granulite-facies overprint following exhumation to lower or middle crustal levels during the Variscan Orogeny. Pseudosection calculations for felsic rocks in the Kutná Hora Complex (Fig. 7) indicate that most of the reactions between minerals occurred below 1·5 GPa and 500°C, where up to 7 vol. % of garnet was formed. Important information deduced from the pseudosection is that only 2 vol. % of garnet formed at UHP conditions and that no garnet was produced during decompression or cooling. The growth of new garnet during the second event will occur in an environment with higher Y + REE concentrations, resulting in the formation of an annulus. When comparing the distribution of Y + HREE in the felsic granulite from the Kutná Hora Complex (Fig. 9j and k) with those in the literature (Fig. 9), the garnet from the felsic granulite shows higher values of Y + HREE in the annular maximum than in the core. This suggests high concentrations of Y + REE in the matrix that, owing to changing *P–T* conditions, were incorporated in the new garnet. However, this does not rule out the effect of other factors, as described above, that could control the overall distribution of Y + REE in garnet. This includes small-scale irregularities or fluctuations in Y + REE concentrations that could relate to the breakdown of former accessory phases or pre-existing heterogeneities in the matrix during crystal growth (Yang & Rivers, 2002; Hirsch *et al.*, 2003; Yang & Pattison, 2006). The best example is patchy and irregular phosphorus zoning in Fig. 5d. The different concentrations of trace elements on the opposite sides of the garnet also signify grain-scale disequilibrium partitioning or uptake of trace elements limited by rates of intergranular diffusion (Skora *et al.*, 2006). It should be noted that apart from apatite, no Y- and REE-bearing accessory phase was observed in garnet.

The granulite-facies overprint has been assumed to occur by nearly isobaric heating as the result of asthenospheric upwelling and intrusion of ultramafic magma in the Moldanubian crust (Faryad *et al.*, 2015). According to the pseudosection modeling, proportionally 5 vol. % garnet was formed during granulite-facies metamorphism, whereas the other 9 vol. % is related to the UHP event. Because of diffusion during the granulite-facies event the exact boundary of these two garnets cannot be estimated owing to possible partial resorption of UHP garnet and diffusion modification. Quantitative determinations of rates of diffusion of Y and REE from partially resorbed garnet crystals by Carlson (2012) showed significant change at the outermost rims of garnets. Whereas Nd, Sm, and Eu are strongly depleted in the rims of relict garnet crystals owing to preferential partitioning out of garnet during resorption, Y and some other REE (Er, Tm, Yb, Lu, Tb, Dy, Ho) are strongly concentrated in the relict garnet rims by resorption. Therefore partial increase of Y and HREE at the rim of UHP garnet could occur by its resorption during exhumation. Figure 10 shows the distribution of REE [normalized to chondrite after Anders & Grevasse (1989)] in bulk-rocks and in garnet from the studied samples. Sample F103-10 has markedly lower REE contents that are probably due to the presence of thin layers of quartz and K-feldspar. The REE content of sample RJ30-13, which has a mineral assemblage similar to that of sample F103-10, is also plotted for comparison. There is generally a decrease, mainly of HREE, from core to rim. All three analysed garnet grains show negative europium anomalies that reflect the overall bulk-rock composition. However, a slight change in Eu anomaly is visible between the core and rim of garnet in sample RJ34-13 (Fig. 10a and b). Considering formation of the garnet rim during the granulite-facies stage, this change in the Eu anomaly could be due to simultaneous crystallization of garnet and plagioclase or ternary feldspar. The pseudosection in Fig. 8a indicates the presence of plagioclase with garnet at temperatures below 650°C, but above this temperature limit two feldspars are stable owing to the inclusion of the melt model in the calculation. The two feldspars are represented here by ternary feldspar.

Phosphorus zoning in garnet

Apatite is a common phosphate phase in eclogite-facies rocks, although moderate amounts of P can enter garnet as pressure and temperature increases (Konzett & Frost, 2009). Because phosphorus diffusion in garnet is

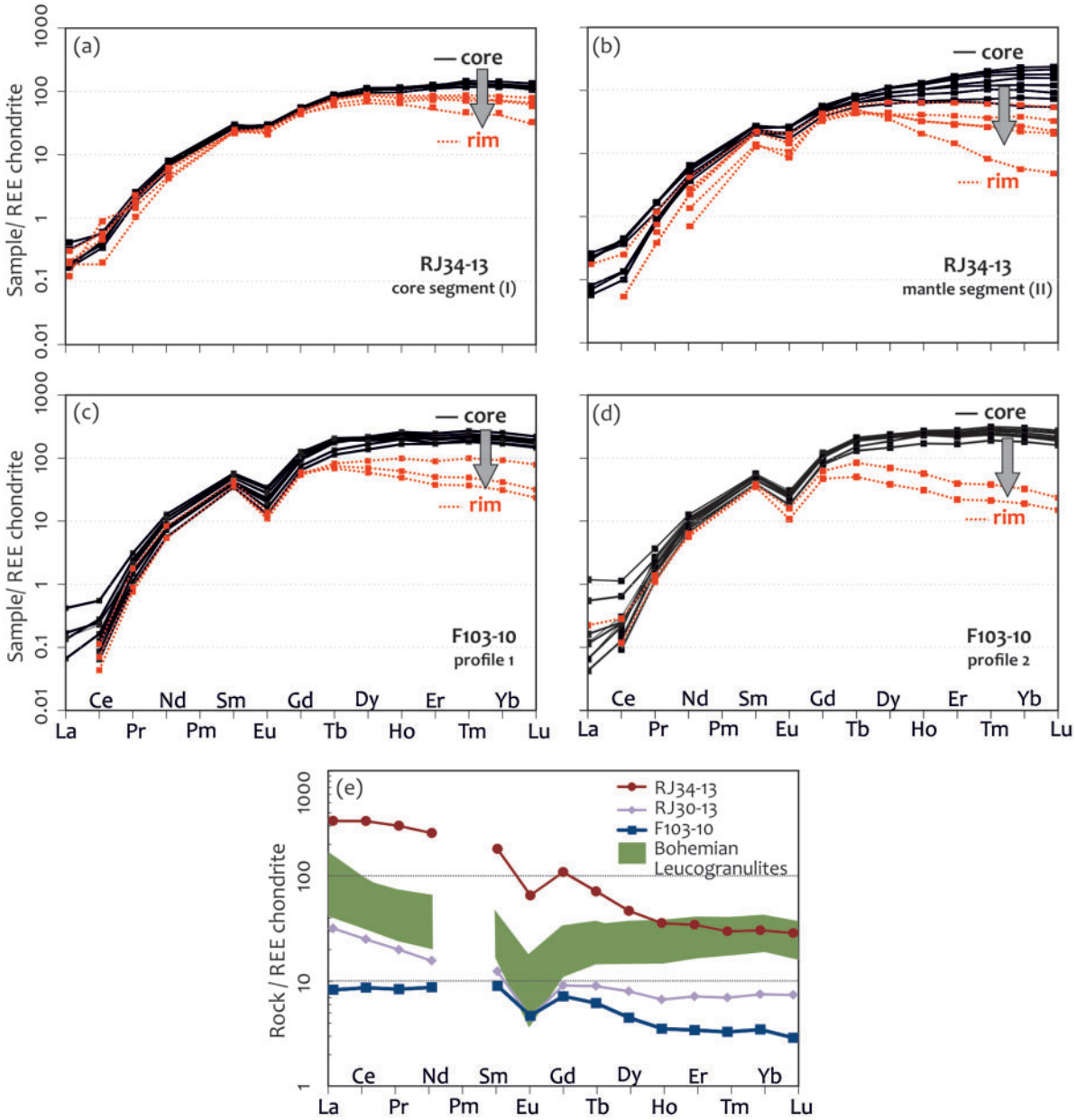

Fig. 10. Chondrite-normalized REE patterns [chondrite values after Anders & Grevasse (1989)] in the studied garnets from mesocratic and leucocratic layers of the granulite. (a, b) REE patterns for the core and mantle of garnet in sample RJ34-13 are indicated separately; (c, d) REE patterns for two separate grains in sample F103-10; (e) bulk-rock REE patterns of granulite from the Kutná Hora Complex (RJ34-13, F103-10 and RJ30-13). REE patterns for the South Bohemian granulite (Kotková & Harley, 2010) are also shown for comparison.

slow, phosphorus distribution in garnet can help to decipher its growth history; for example, through preserved growth zones as described by Vielzeuf *et al.* (2005). By investigating high-grade metapelites containing a sub-solidus assemblage with garnet, Spear & Kohn (1996) showed that phosphorus may increase at the rim of garnet grains, reflecting increased participation of apatite as melting progressed. According to Kawakami & Hokada (2010), the P enrichment in garnet rims from high-grade gneiss in the Lützow–Holm Complex (East Antarctica) was the result of resorption–reprecipitation of garnet during melt formation.

One of the most interesting features of the garnet in sample RJ34-13 is the P zoning, particularly at its rims. Detailed compositional maps indicate weak P zoning in the central part and three domains with elevated P concentrations. As mentioned above, apatite is rarely present as an inclusion in garnet, but occurs in the matrix, mainly in direct contact with garnet rims or within intergranular spaces of garnet clusters. Therefore the three domains could be the result of P diffusion from apatite inclusions below the host garnet surface. According to Brunet *et al.* (2006), Si–P exchange in garnet under UHP conditions occurs by the $MgPAl_{-1}Si_{-1}$ substitution. The

presence of monazite in the matrix (Fig. 3a) as a P-bearing phase can also have influenced P zoning in the garnet rim. In contrast to irregular P zoning at the rim of garnet, the zoning in the central part of the garnet crystal follows its crystallographic planes. This may suggest that the central zoning was a result of continuous garnet crystallization during eclogite-facies metamorphism, whereas the rim part was formed after a possible growth gap during granulite-facies metamorphism in the presence of a melt. The older eclogite-facies garnet that was partly replaced or consumed by matrix phases during exhumation was overgrown by a new P-bearing garnet.

P–T history of felsic granulite from the Kutná Hora Complex and implications for HP–UHP and subsequent granulite-facies metamorphism in the Moldanubian Zone

The trace element distribution patterns in garnet, in combination with thermodynamic modeling, in the felsic granulites from the Kutná Hora Complex support the interpretation of two separate Variscan metamorphic events in the Moldanubian Zone (Faryad & Fišera, 2015; Faryad *et al.*, 2015). From the garnet composition, these two events are recorded by the high Y and HREE contents in the core and in the mantle (annulus) part, suggesting nucleation and growth of the first and second garnet, respectively. From the pseudosection modeling, mainly based on grossular isopleths, we interpret that the first garnet was formed during a prograde *P–T* path from pressure and temperature conditions below 0·6 GPa and 400°C (Fig. 7b) to 3·2–4·0 GPa at about 700°C (path 1 in Fig. 11). As the initial profiles of major elements in garnet grains, including calcium contents, were modified to various degrees by diffusion, the intersection of Grs and X_{Fe} isopleth values indicate only an approximate *P–T* condition for the garnet core, whereas the real values for garnet nucleation were based on pseudosection modeling at even lower pressures and temperatures. However, UHP conditions for these granulites were recently confirmed by the finding of micro-diamond and coesite (Perraki & Faryad, 2014). Modal volume calculations of garnet indicate continuous growth during this UHP event that reached 9 vol. % in the coesite and diamond stability fields (Fig. 7).

There are two alternative scenarios to explain the exhumation of felsic rocks from mantle depths and their subsequent granulite-facies metamorphism that could produce the second garnet. The first is decompression and heating to granulite-facies conditions of 1·5–2·0 GPa at 800–1000°C as estimated for the felsic granulite in the Moldanubian Zone (paths a, b and c in Fig. 11). However, such a *P–T* path will, based on the volume calculations, produce no garnet, even if the rocks are first heated at UHP conditions and then decompressed at high temperatures to granulite-facies conditions (Fig. 8). In addition, an isothermal decompression to the granulite-facies stage would result in

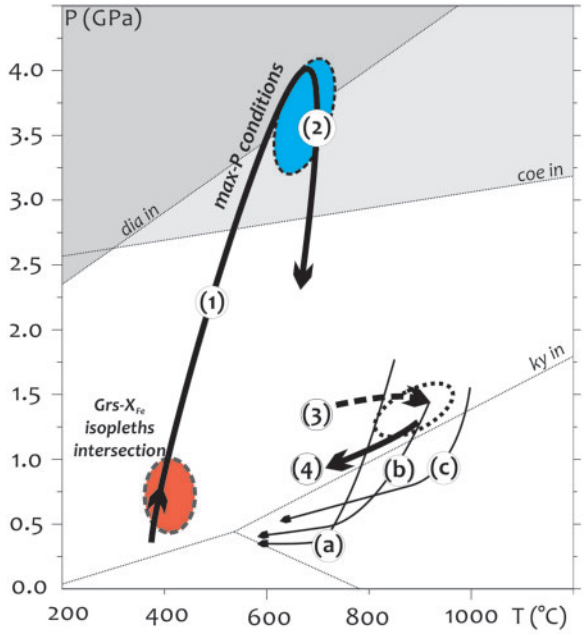

Fig. 11. Inferred *P–T* paths of the HP granulites in the Moldanubian Zone, based on compositional zoning of garnet and calculated pressure and temperature conditions from the Kutná Hora granulites. (1) Prograde stage reaching UHP conditions. The ellipses indicate *P–T* fields based on intersection of garnet isopleths for the core and mantle composition of garnet in combination with the data of Perraki & Faryad (2014). It should be noted that garnet nucleates at even lower *P–T* conditions (see Fig. 7). (2) Exhumation stage to lower crustal levels. (3, 4) Heating and cooling back during the granulite-facies overprint for the Kutná Hora felsic granulite, obtained in this study. The cooling and exhumation *P–T* paths (a–c) of the Moldanubian granulites from different crustal positions are from (a) Strážek Unit (Tajčmanová *et al.*, 2006), (b) South Bohemian granulites (Vrána, 1992; Kotková & Harley, 1999) and (c) granulites of Lower Austria (Carswell & O'Brien, 1993).

total homogenization of the prograde compositional zoning in garnet (Chakraborty & Ganguly, 1992; Carlson, 2006; Vielzeuf *et al.*, 2005), unless the exhumation rate from mantle depths to crustal levels was too fast. The second model is an isothermal decompression from UHP conditions at intermediate temperature (path 2 in Fig. 11). After the rocks were exhumed to lower or middle crustal levels, they were subjected to heating at granulite-facies conditions (path 3 in Fig. 11). The high peak of Y and HREE concentrations can be the result of partial decomposition of the first garnet during exhumation, during which the trace elements released into the matrix participated in the formation of new garnet. Such a model for granulite-facies metamorphism in the Moldanubian Zone has been explained by slab break-off and mantle upwelling as a potential heat source for the granulite-facies metamorphism (Faryad *et al.*, 2015). This process was followed by the formation of huge volumes of granitoid magma and their intrusion within the Moldanubian Plutonic Complex (Žák *et al.*, 2014).

In addition to preservation of prograde zoned garnet, the two separate metamorphic events recorded by the felsic granulites can also explain the wide range of age

determinations for the felsic granulites and their associated mafic and ultramafic bodies (e.g. Schulmann *et al.*, 2005). Most U–Pb age data on zircon from granulites indicate an age of about 340 Ma that is generally accepted as the culmination of granulite-facies metamorphism. However, there are a number of older ages; for example, Sm–Nd ages on garnet of 370–390 Ma from garnet peridotite and pyroxenite (Beard *et al.*, 1992) or of 360 Ma from felsic granulites (Prince *et al.*, 2000), and U–Pb zircon ages of 359–380 Ma from felsic granulites (Teipel *et al.*, 2012; Nahodilová *et al.*, 2014). The older ages are interpreted to date the HP–UHP event, whereas the granulite-facies metamorphism occurred at around 340 Ma (Faryad, 2011). The relationship of the granulite-facies metamorphism to younger mafic and ultramafic intrusions in the Moldanubian Zone is assumed based on U–Pb age dating on zircon from a metatroctolite with granulite-facies coronas around olivine (Faryad *et al.*, 2015).

CONCLUSIONS

Major and trace element compositional zoning in garnet from felsic granulites in the Kutná Hora Complex (Moldanubian Zone) demonstrates that the rocks experienced two metamorphic events. The first metamorphism occurred in a subduction-zone setting and the second at deep crustal levels, constrained by the following findings.

1. Major element prograde zoning is preserved in the cores of garnets. Thermodynamic modeling indicates that both subduction that reached UHP conditions and subsequent exhumation occurred at relatively low temperatures (below 650–700°C). These allowed the preservation of prograde zoning, including bell-shaped Mn and Y + HREE profiles in garnet cores.
2. Annular peaks of Y + HREE, developed in the mantle part of garnet crystals, are interpreted as the result of granulite-facies metamorphism that mostly occurred in deeper crustal levels. In addition to Y + REE-bearing mineral reactions and partitioning of these elements into garnet during an increase of temperature, the high annular peaks are interpreted to be the result of partial resorption of HP–UHP garnet and the release of trace elements into the matrix during exhumation, followed by their incorporation back into the new garnet during the granulite-facies event.
3. The preservation of prograde zoning in garnet, which experienced UHP and subsequent granulite-facies metamorphism, suggests that the tectonic and metamorphic processes that occurred during continental collision were too fast to result in total homogenization of the garnet in the felsic rocks.
4. The results of this study support a tectonic model suggesting a short-lived granulite-facies overprint that is assumed to have been caused by break-off of the subducting slab and mantle upwelling during the Variscan Orogeny in the Moldanubian Zone.

ACKNOWLEDGEMENTS

The authors thank K. Ettinger and M. Racek for their help with microprobe analyses. We greatly appreciate the constructive reviews by J. F. Otamendi, J. Kotková and an anonymous reviewer. Careful editorial comments of A. Skelton substantially improved the paper.

FUNDING

This work was supported by the Czech Science Foundation (research project number 13-06958S).

SUPPLEMENTARY DATA

Supplementary data for this paper are available at *Journal of Petrology* online.

REFERENCES

Anders, E. & Grevasse, N. (1989). Abundance of the elements: Meteoritic and Solar. *Geochimica et Cosmochimica Acta* **53**, 197–214.

Anderson, D. E. & Buckley, G. R. (1973). Zoning in garnets: Diffusion models. *Contributions to Mineralogy and Petrology* **40**, 87–104.

Beard, B. L., Medaris, L. G., Johnson, C. M., Brueckner, H. K. & Mísař, Z. (1992). Petrogenesis of Variscan high-temperature group-A eclogites from the Moldanubian zone of the Bohemian Massif, Czechoslovakia. *Contributions to Mineralogy and Petrology* **111**, 468–483.

Benisek, A., Dachs, E. & Kroll, H. (2010). A ternary feldspar-mixing model based on calorimetric data: development and application. *Contributions to Mineralogy and Petrology* **160**, 327–337.

Bhattacharya, A., Mohanty, L., Maji, A., Sen, S. K. & Raith, M. (1992). Non-ideal mixing in the phlogopite–annite binary: constraints from experimental data on Mg–Fe partitioning and a reformulation of the biotite–garnet geothermometer. *Contributions to Mineralogy and Petrology* **111**, 87–93.

Blackburn, W. H. & Navarro, E. (1977). Garnet zoning and polymetamorphism in the eclogitic rocks of Isla de Margarita, Venezuela. *Canadian Mineralogist* **15**, 257–266.

Brunet, F., Bonneau, V. & Irifune, T. (2006). Complete solid-solution between $Na_3Al_2(PO_4)_3$ and $Mg_3Al_2(SiO_4)_3$ garnets at high pressure. *American Mineralogist* **91**, 211–215.

Carlson, W. D. (1989). The significance of intergranular diffusion to the mechanisms and kinetics of porphyroblast crystallization. *Contributions to Mineralogy and Petrology* **103**, 1–24.

Carlson, W. D. (2006). Rates of Fe, Mg, Mn, and Ca diffusion in garnet. *American Mineralogist* **91**, 1–11.

Carlson, W. D. (2012). Rates and mechanism of Y, REE and Cr diffusion in garnet. *American Mineralogist* **97**, 1598–1618.

Carlson, W. D., Gale, J. D. & Wright, K. (2014). Incorporation of Y and REEs in aluminosilicate garnet: Energetics from atomistic simulation. *American Mineralogist* **99**, 1022–1034.

Carswell, D. A. & O'Brien, P. J. (1993). Thermobarometry and geotectonic significance of high-pressure granulites: examples from the Moldanubian zone of the Bohemian Massif in Lower Austria. *Journal of Petrology* **34**, 427–459.

Cháb, J., Stráník, Z. & Eliáš, M. (2007). *Geologická mapa České republiky 1:500.000*. Česká geologická služba.

Chakraborty, S. & Ganguly, J. (1992). Cation diffusion in aluminosilicate garnets: Experimental determination in spessartine–almandine diffusion couples, evaluation of effective binary diffusion coefficients, and applications. *Contributions to Mineralogy and Petrology* **111**, 74–86.

Chamberlain, C. P. & Conrad, M. E. (1993). Oxygen-isotope zoning in garnet: A record of volatile transport. *Geochimica et Cosmochimica Acta* **57**, 2613–2629.

Cheng, H., Nakamura, E., Kobayashi, K. & Zhou, Z. (2007). Origin of atoll garnets in eclogites and implications for the redistribution of trace elements during slab exhumation in a continental subduction zone. *American Mineralogist* **92**, 1119–1129.

Chernoff, C. B. & Carlson, W. D. (1999). Trace element zoning as a record of chemical disequilibrium during garnet growth. *Geology* **27**, 555–558.

Coggon, R. & Holland, T. J. B. (2002). Mixing properties of phengitic micas and revised garnet–phengite thermobarometers. *Journal of Metamorphic Geology* **20**, 683–696.

Connolly, J. A. D. (2005). Computation of phase-equilibria by linear programming: a tool for geodynamic modeling and its application to subduction zone decarbonation. *Earth and Planetary Science Letters* **236**, 524–541.

Cygan, R. T. & Lasaga, A. C. (1982). Crystal-growth and the formation of chemical zoning in garnets. *Contributions to Mineralogy and Petrology* **79**, 187–200.

Dallmeyer, R. D., Franke, W. & Weber, K. (1995). *Pre-Permian Geology of Central and Eastern Europe*. Springer, 593 pp.

Dasgupta, S., Sengupta, P., Guha, D. & Fukuoka, M. (1991). A refined garnet–biotite Fe–Mg exchange geothermometer and its application in amphibolites and granulites. *Contributions to Mineralogy and Petrology* **109**, 130–137.

Dawson, J. B. & Carswell, D. A. (1990). High-temperature and ultra-high-pressure eclogites. In: Carswell, D. A. (ed.) *Eclogite Facies Rocks*. Blackie, pp. 314–349.

Erambert, M. & Austrheim, H. (1993). The effect of fluid and deformation on zoning and inclusion patterns in poly-metamorphic garnets. *Contributions to Mineralogy and Petrology* **115**, 204–214.

Faryad, S. W. (2009). The Kutná Hora Complex (Moldanubian zone, Bohemian Massif): A composite of crustal and mantle rocks subducted to HP/UHP conditions. *Lithos* **109**, 193–208.

Faryad, S. W. (2011). Distribution and geological position of high-/ultrahigh-pressure units within the European Variscan Belt: a review. In: Dobrzhinetskaya, L., Faryad, S.W., Wallis, S. & Cuthbert, S. (eds) *Ultrahigh Pressure Metamorphism: 25 Years After the Discovery of Coesite and Diamond*. Elsevier, pp. 361–397.

Faryad, S. W. (2012). High-pressure polymetamorphic garnet growth in eclogites from the Mariánské Lázně Complex (Bohemian Massif). *European Journal of Mineralogy* **24**, 483–497.

Faryad, S. W. & Chakraborty, S. (2005). Duration of Eo-Alpine metamorphic event obtained from multicomponent diffusion modeling of garnet: A case study from the Eastern Alps. *Contributions to Mineralogy and Petrology* **150**, 305–318.

Faryad, S. W. & Fišera, M. (2015). Olivine-bearing symplectites in fractured garnet from eclogite, Moldanubian Zone (Bohemian Massif)—a short-lived, granulite facies event. *Journal of Metamorphic Geology* **33**, 597–612.

Faryad, S. W. & Kachlík, V. (2013). New evidence of blueschist facies rocks and their geotectonic implication for Variscan suture(s) in the Bohemian Massif. *Journal of Metamorphic Geology* **31**, 63–82.

Faryad, S. W., Dolejš, D. & Machek, M. (2009). Garnet exsolution in pyroxene from clinopyroxenites in the Moldanubian zone: constraining the early pre-convergence history of ultramafic rocks in the Variscan orogen. *Journal of Metamorphic Geology* **27**, 655–671.

Faryad, S. W., Klápová, H. & Nosál, L. (2010a). Mechanism of formation of atoll garnet during high-pressure metamorphism. *Mineralogical Magazine* **74**, 111–126.

Faryad, S. W., Nahodilová, R. & Dolejš, D. (2010b). Incipient eclogite facies metamorphism in the Moldanubian granulites revealed by mineral inclusions in garnet. *Lithos* **114**, 54–69.

Faryad, S. W., Kachlík, V., Sláma, J. & Hoinkes, G. (2015). Implication of corona formation in a metatroctolite to the granulite facies overprint of HP–UHP rocks in the Moldanubian zone (Bohemian Massif). *Journal of Metamorphic Geology* **33**, 295–310.

Franke, W. (2000). The mid-European segment of the Variscides: tectonostratigraphic units, terranes, boundaries and plate evolution. In: Franke, W., Haak, V., Oncken, O. & Tanner, D. (eds) *Orogenic Processes: Quantification and Modelling in the Variscan Belt. Geological Society, London, Special Publications* **179**, 35–61.

Ganguly, J. & Saxena, S. K. (1984). Mixing properties of alumino-silicate garnets: constraints from natural and experimental data, and applications to geothermometry. *American Mineralogist* **69**, 88–97.

Hickmott, D. D. & Shimizu, N. (1989). Trace element zoning in garnet from Kwoiek area, British Columbia: disequilibrium partitioning during garnet growth? *Contributions to Mineralogy and Petrology* **104**, 619–630.

Hickmott, D. D. & Spear, F. S. (1992). Major- and trace-element zoning in garnets from calcareous pelites in the NW Shelburne Falls quadrangle, Massachusetts: garnet growth histories in retrograded rocks. *Journal of Petrology* **33**, 965–1005.

Hickmott, D. D., Shimizu, N., Spear, F. S. & Selverstone, J. (1987). Trace-element zoning in a metamorphic garnet. *Geology* **15**, 573–576.

Hirsch, D. M., Prior, D. J. & Carlson, W. D. (2003). An overgrown model to explain multiple dispersed high-Mn regions in the cores of garnet porphyroblasts. *American Mineralogist* **88**, 131–141.

Hodges, K. V. & Crowley, P. D. (1985). Error estimation in empirical geothermometry and geobarometry for pelitic systems. *American Mineralogist* **70**, 702–709.

Hodges, K. V. & Spear, F. S. (1982). Geothermometry, geobarometry and the Al_2SiO_5 triple point at Mt Mooslanke, New Hampshire. *American Mineralogist* **67**, 1118–1134.

Holdaway, M. J. (2000). Application of new experimental and garnet Margules data to the garnet–biotite geothermometer. *American Mineralogist* **85**, 881–892.

Holland, T. J. B. & Powell, R. (1996). Thermodynamics of order–disorder in minerals. 2. Symmetric formalism applied to solid solutions. *American Mineralogist* **81**, 1425–1437.

Holland, T. J. B. & Powell, R. (1998). An internally consistent thermodynamic data set for phases of petrological interest. *Journal of Metamorphic Geology* **16**, 309–343.

Holland, T. J. B. & Powell, R. (2001). Calculation of phase relations involving haplogranitic melts using an internally consistent thermodynamic dataset. *Journal of Petrology* **42**, 673–683.

Holland, T., Baker, J. & Powell, R. (1998). Mixing properties and activity–composition relationships of chlorites in the system

MgO–FeO–Al_2O_3–SiO_2–H_2O. *European Journal of Mineralogy* **10**, 395–406.

Hollister, L. S. (1966). Garnet zoning: an interpretation based on the Rayleigh fractionation model. *Science* **154**, 1647–1651.

Jakeš, P. (1997). Melting in high-*P* region—case of Bohemian granulites. *Acta Universitatis Carolinae, Geologica* **41**, 113–125.

Jamtveit, B., Wogelius, R. A. & Fraser, D. G. (1993). Zonation patterns of skarn garnets: Records of hydrothermal system evolution. *Geology* **21**, 113–116.

Janoušek, V., Finger, F., Roberts, M. P., Frýda, J., Pin, C. & Dolejš, D. (2004). Deciphering petrogenesis of deeply buried granites: whole-rock geochemical constraints on the origin of largely undepleted felsic granulites from the Moldanubian Zone of the Bohemian Massif. *Transactions of the Royal Society of Edinburgh, Earth Sciences* **95**, 141–154.

Jochum, K. P., Weis, U., Stoll, B., Kuzmin, D., Yang, Q., Raczek, I., Jacob, D. E., Stracke, A., Birbaum, K., Frick, D. A., Günther, D. & Enzweiler, J. (2011). Determination of reference values for NIST SRM 610–617 glasses following ISO guidelines. *Geostandards and Geoanalytical Research* **35**, 397–429.

Kawakami, T. & Hokada, T. (2010). Linking *P–T* path with development of discontinuous phosphorus zoning in garnet during high-temperature metamorphism—an example from Lützow–Holm Complex, East Antarctica. *Journal of Mineralogical and Petrological Sciences* **105**, 175–186.

Kohn, M. J. & Spear, F. (2000). Retrograde net transfer reaction insurance for pressure–temperature estimates. *Geology* **28**, 1127–1130.

Konrad-Schmolke, M., O'Brien, P. J., De Capitani, C. & Carswell, D. A. (2008a). Garnet growth at high- and ultra-high-pressure conditions and the effect of element fractionation on mineral modes and composition. *Lithos* **103**, 309–332.

Konrad-Schmolke, M., Zack, T., O'Brien, P. J. & Jacob, D. E. (2008b). Combined thermodynamic and rare earth element modelling of garnet growth during subduction: Examples from ultrahigh-pressure eclogite of the Western Gneiss Region, Norway. *Earth and Planetary Science Letters* **272**, 488–498.

Konzett, J. & Frost, D. (2009). The high *P–T* stability of hydroxyl-apatite in natural and simplified MORB—an experimental study to 15 GPa with implications for transport and storage of phosphorus and halogens in subduction zones. *Journal of Petrology* **50**, 2043–2062.

Kotková, J. (2007). High-pressure granulites of the Bohemian Massif: recent advances and open questions. *Journal of Geosciences* **52**, 45–71.

Kotková, J. & Harley, S. L. (1999). Formation and evolution of high-pressure leucogranulites: experimental constraints and unresolved issues. *Physics and Chemistry of the Earth, Part A* **24**, 299–304.

Kotková, J. & Harley, S. L. (2010). Anatexis during high-pressure crustal metamorphism: evidence from garnet–whole-rock REE relationships and zircon–rutile Ti–Zr thermometry in leucogranulites from the Bohemian Massif. *Journal of Petrology* **51**, 1967–2001.

Koziol, A. M. (1989). Recalibration of the garnet–plagioclase–Al_2SiO_5–quartz (GASP) geobarometer and applications for natural parageneses. *EOS Transactions, American Geophysical Union* **70**, 493.

Lanzirotti, A. (1995). Yttrium zoning in metamorphic garnets. *Geochimica et Cosmochimica Acta* **59**, 4105–4110.

Medaris, L. G., Jelínek, E. & Mísař, Z. (1995). Czech eclogites—Terrane settings and implications for Variscan tectonic evolution of the Bohemian Massif. *European Journal of Mineralogy* **7**, 7–28.

Medaris, L. G., Beard, B. L. & Jelínek, E. (2006). Mantle-derived, UHP garnet pyroxenite and eclogite in the Moldanubian Gföhl Nappe, Bohemian Massif: a geochemical review, new *P–T* determinations and tectonic interpretation. *International Geology Review* **48**, 765–777.

Moore, S. J., Carlson, W. D. & Hesse, M. A. (2013). Origins of yttrium and rare earth element distributions in metamorphic garnet. *Journal of Metamorphic Geology* **31**, 663–689.

Nahodilová, R., Faryad, S. W., Dolejš, D., Tropper, P. & Konzett, J. (2011). High-pressure partial melting and melt loss in felsic granulites in the Kutná Hora complex, Bohemian Massif (Czech Republic). *Lithos* **125**, 641–658.

Nahodilová, R., Štípská, P., Powell, R., Košler, J. & Racek, M. (2014). High-Ti muscovite as a prograde relict in high pressure granulites with metamorphic Devonian zircon ages (Běstvina granulite body, Bohemian Massif): Consequence for the relamination model of subducted crust. *Gondwana Research* **25**, 630–648.

Newton, R. C., Charlu, T. V. & Kleppa, O. J. (1980). Thermochemistry of the high structural state plagioclases. *Geochimica et Cosmochimica Acta* **44**, 933–941.

Otamendi, J. E., de la Rosa, J. D., Patiño Douce, A. E. & Castro, A. (2002). Rayleigh fractionation of heavy rare earths and yttrium during metamorphic garnet growth. *Geology* **30**, 159–162.

Perchuk, L. L. & Lavrent'eva, L. Y. (1983). Experimental investigation of exchange equilibria in the system cordierite–garnet–biotite. In: Saxena, S. K. (ed.) *Kinetics and Equilibrium in Mineral Reactions. Advances in Physical Geochemistry* **3**, 199–239.

Perraki, M. & Faryad, S. W. (2014). First finding of microdiamond, coesite and other UHP phases in felsic granulites in the Moldanubian Zone: Implications for deep subduction and a revised geodynamic model for Variscan Orogeny in the Bohemian Massif. *Lithos* **202–203**, 157–166.

Pouba, Z., Fiala, J. & Paděra, K. (1987). The granulite body near Běstvina in the Železné Hory Mts. *Časopis pro Mineralogii a Geologii* **32**, 73–78.

Powell, R. & Holland, T. J. B. (1999). Relating formulations of the thermodynamics of mineral solid solutions: Activity modeling of pyroxenes, amphiboles, and micas. *American Mineralogist* **84**, 1–14.

Powell, R., Holland, T. & Worley, B. (1998). Calculating phase diagrams involving solid solutions via non-linear equations, with examples using THERMOCALC. *Journal of Metamorphic Geology* **16**, 577–588.

Prince, C. I., Košler, J., Vance, D. & Günther, D. (2000). Comparison of laser ablation ICP-MS and isotope dilution REE analyses—implications for Sm–Nd garnet geochronology. *Chemical Geology* **168**, 255–274.

Proyer, A. (2003). The preservation of high pressure rocks during exhumation: metagranites and metapelites. *Lithos* **70**, 183–194.

Pyle, J. M. & Spear, F. S. (1999). Yttrium zoning in garnet: Coupling of major and accessory phases during metamorphic reactions. *Geological Materials Research* **1**, 1–49.

Schulmann, K., Kröner, A., Hegner, E., Wendt, I., Konopásek, J., Lexa, O. & Štípská, P. (2005). Chronological constraints on the pre-orogenic history, burial and exhumation of deep-seated rocks along the eastern margin of the Variscan Orogen, Bohemian Massif, Czech Republic. *American Journal of Science* **305**, 407–448.

Schwandt, C. S., Papike, J. J. & Shearer, C. K. (1996). Trace element zoning in pelitic garnet of the Black Hills, South Dakota. *American Mineralogist* **81**, 1195–1207.

Skora, S., Baumgartner, L. P., Mahlen, N. J., Johnson, C. M., Pilet, S. & Hellebrand, E. (2006). Diffusion-limited REE uptake by eclogite garnets and its consequences for Lu–Hf and Sm–Nd geochronology. *Contributions to Mineralogy and Petrology* **152**, 703–720.

Spear, F. S. (1988). Thermodynamic projection and extrapolation of high-variance mineral assemblages. *Contributions to Mineralogy and Petrology* **98**, 346–351.

Spear, F. S. & Kohn, M. J. (1996). Trace element zoning in garnet as a monitor of crustal melting. *Geology* **24**, 1099–1102.

Strnad, L., Mihaljević, M. & Šebek, O. (2005). Laser ablation and solution ICP-MS determination of REE in USGS BIR-1G, BHVO-2G and BCR-2G glass reference materials. *Geostandards and Geoanalytical Research* **29**, 303–314.

Stüwe, K. (1997). Effective bulk composition changes due to cooling: a model predicting complexities in retrograde reaction textures. *Contributions to Mineralogy and Petrology* **129**, 43–52.

Synek, J. & Oliveriová, D. (1993). Terrane character of the northeast margin of the Moldanubian Zone—the Kutná Hora crystalline complex, Bohemian Massif. *Geologische Rundschau* **82**, 566–582.

Tajćmanová, L., Konopásek, J. & Schulmann, K. (2006). Thermal evolution of the orogenic lower crust during exhumation within a thickened Moldanubian root of the Variscan belt of Central Europe. *Journal of Metamorphic Geology* **24**, 119–134.

Teipel, U., Finger, F. & Rohrmüller, J. (2012). Remnants of Moldanubian HP–HT granulites in the eastern part of the Bavarian Forest (southwestern Bohemian Massif); evidence from SHRIMP zircon dating and whole rock geochemistry. *Zeitschrift der Deutschen Gesellschaft für Geowissenschaften* **163**, 137–152.

Tracy, R. J. (1982). Compositional zoning and inclusions in metamorphic minerals. In: Ferry, J. M. (ed.) *Characterization of Metamorphism through Mineral Equilibria. Mineralogical Society of America, Reviews in Mineralogy* **10**, 355–397.

Tracy, R. J., Robinson, P. & Thompson, A. B. (1976). Garnet composition and zoning in the determination of temperature and pressure of metamorphism, central Massachusetts. *American Mineralogist* **61**, 762–775.

Vielzeuf, D., Veschambre, M. & Brunet, F. (2005). Oxygen isotope heterogeneities and diffusion profile in composite metamorphic–magmatic garnets from the Pyrenees. *American Mineralogist* **90**, 463–472.

Vrána, S. (1992). The Moldanubian Zone in southern Bohemia: Polyphase evolution of imbricated crustal and upper mantle segments. In: Kukal, Z. (ed.) *Proceedings of the 1st International Conference on the Bohemian Massif, Prague, September 26-October 3, 1988*. Czech Geological Survey, Prague, pp. 331–335.

Vrána, S., Štědrá, V. & Fišera, M. (2005). Petrology and geochemistry of the Běstvina granulite body metamorphosed at eclogite facies conditions, Bohemian Massif. *Journal of the Czech Geological Society* **50**, 95–106.

Whitney, D. L. & Evans, B. W. (2010). Abbreviations for names of rock-forming minerals. *American Mineralogist* **95**, 185–187.

Willner, A. P., Sebazungu, E., Gerya, T. V., Maresch, W. V. & Krohe, A. (2002). Numerical modelling of PT-paths related to rapid exhumation of high-pressure rocks from the crustal root in the Variscan Erzgebirge Dome (Saxony/Germany). *Journal of Geodynamics* **33**, 281–314.

Yang, P. & Pattison, D. (2006). Genesis of monazite and Y zoning in garnet from the Black Hills, South Dakota. *Lithos* **88**, 233–253.

Yang, P. & Rivers, T. (2002). The origin of Mn and Y annuli in garnet and the thermal dependence of P in garnet and Y in apatite in calcpelite and pelite, Gagnon terrane, western Labrador. *Geological Materials Research* **4**, 1–35.

Young, E. D. & Rumble, D. (1993). The origin of correlated variations in *in-situ* $^{18}O/^{16}O$ and elemental concentrations in metamorphic garnet from southeastern Vermont, USA. *Geochimica et Cosmochimica Acta* **57**, 2585–2597.

Žák, J., Verner, K., Janoušek, V., Holub, F. V., Kachlík, V., Finger, F., Hajná, J., Tomek, F., Vondrovic, L. & Trubać, J. (2014). A plate-kinematic model for the assembly of the Bohemian Massif constrained by structural relations around granitoid plutons. In: Schulmann, K., Martínez Catalán, J. R., Lardeaux, J. M., Janoušek, V. & Oggiano, G. (eds) *The Variscan Orogeny: Extent, Timescale and the Formation of the European Crust. Geological Society, London, Special Publications* **405**, 169–196.